AUSTIN CHALK FRACTURE MAPPING USING FREQUENCY

DATA DERIVED FROM SEISMIC DATA

A Dissertation

by

ILYAS JUZER NAJMUDDIN

Submitted to the Office of Graduate Studies of
Texas A&M University
in partial fulfillment of the requirements for the degree of

DOCTOR OF PHILOSOPHY

May 2003

Major Subject: Geophysics

AUSTIN CHALK FRACTURE MAPPING USING FREQUENCY

DATA DERIVED FROM SEISMIC DATA

A Dissertation

by

ILYAS JUZER NAJMUDDIN

Submitted to Texas A&M University
in partial fulfillment of the requirements
for the degree of

DOCTOR OF PHILOSOPHY

Approved as to style and content by:

Joel S. Watkins (Chair of Committee)	Richard L. Gibson (Member)
Robert R. Berg (Member)	Anthony F. Gangi (Member)
Maria A. Barrufet (Member)	Andrew Hajash (Head of Department)

May 2003

Major Subject: Geophysics

ABSTRACT

Austin Chalk Fracture Mapping Using Frequency Data Derived From Seismic

Data. (May 2003)

Ilyas Juzer Najmuddin, B.S., Cairo University;

M.S., University of Houston

Chair of Advisory Committee: Dr. Joel S. Watkins

Frequency amplitude spectra derived from P-wave seismic data can be used to derive a fracture indicator. This fracture indicator can be used to delineate fracture zones in subsurface layers.

Mapping fractures that have no vertical offset is difficult on seismic sections. Fracturing changes the rock properties and therefore the attributes of the seismic data reflecting off the fractured interface and data passing through the fractured layers. Fractures have a scattering effect on seismic energy reflected from the fractured layer. Fractures attenuate amplitudes of higher frequencies in seismic data preferentially than lower frequencies. The amplitude spectrum of the frequencies in the seismic data shifts towards lower frequencies when a spectrum from a time window above the fractured layer is compared with one below the fractured layer. This shift in amplitudes of frequency spectra can be derived from seismic data and used to indicate fracturing. A method is developed to calculate a parameter t* to measure this change

in the frequency spectra for small time windows (100ms) above and below the fractured layer.

The Austin Chalk in South Central Texas is a fractured layer, and it produces hydrocarbons from fracture zones with the layer (Sweet Spots). 2D and 3D P-wave seismic data are used from Burleson and Austin Counties in Texas to derive the t* parameter.

Case studies are presented for 2D data from Burleson County and 3D data from Austin County. The t* parameter mapped on the 3D data shows a predominant fracture trend parallel to strike. The fracture zones have a good correlation with the faults interpreted on the top of Austin Chalk reflector.

Production data in Burleson County (Giddings Field) is a proxy for fracturing. Values of t* mapped on the 2D data have a good correlation with the cumulative production map presented in this study.

DEDICATION

I dedicate this to my parents and grandparents and ask for their prayers always.

I dedicate this to my family for their support and understanding.

ACKNOWLEDGEMENTS

TABLE OF CONTENTS

LIST OF FIGURES

INTRODUCTION

The Late Cretaceous Austin Chalk is an important oil producing formation in Texas. It is a fine-grained, naturally fractured, brittle formation with an orthogonal set of fractures in outcrops. Permeability of the Chalk is poor except where the Chalk has been fractured (Corbett et al. 1987).

Matrix permeabilities for the Chalk typically range from 10 - 50 microdarcies. Hydrocarbons cannot be produced with this low permeability. However, the permeability of the rock can be increased to several 100 millidarcies due to fracturing (Corbett et al. 1987). Therefore successful exploration and production from the Austin Chalk depends on predicting locations of "sweet spots" or areas of concentrated fractures.

The effect of fracturing on Austin Chalk porosity is negligible. The rock matrix porosity at reservoir depths ranges from 2-4% and is generally less than 5% (Friedman and McKiernan, 1995). The increase in porosity due to fracturing is less than 0.25% (Snyder and Craft, 1977).

Data from wells show one set of open fractures at reservoir depths within the Austin Chalk. The fractures are near vertical and sub_parallel to strike. Steep dips prevent

---

This dissertation follows the style and format of Geophysics.

seismic imaging of fractures and affects are too small to be resolved. As a consequence, fractures do not have a direct signature on seismic data.

Attributes derived from seismic data, such as frequency shifts, change in seismic velocities and AVO response, may be applied to help with fracture detection(Anderson et al. 1974, Al-Shuhail 1998). This study discusses the results of frequency shifts due to transmission of seismic energy through the Chalk layer.

The fractured chalk preferentially attenuates higher frequencies, resulting in a downward shift of dominant frequencies. Comparison of the frequency spectra (of the seismic data) from above and below the Chalk shows this attenuation.

A method is developed in this paper to represent frequency attenuation by an attribute value. Frequency spectra are generated over similar time windows from above and below the Chalk. Frequency amplitudes from these spectra are extracted for two frequency values. These frequency amplitudes are then used in the equation to derive the attribute **t*** using the equation below. This equation is derived in the second (Methods) section of this thesis.

$$\ln(A1/A2)(\text{at } f2) - \ln(A1/A2)(\text{at } f1) = (t*2 - t*1)(f2 - f1)$$

$$t^* = (t^*2 - t^*1) = [\ln(A1/A2)(\text{at } f2) - \ln(A1/A2)(\text{at } f1)] / (f2 - f1)$$

The results are validated by a comparison of the t* attribute value and production data in Burleson County. Results from 3D seismic data set are consistent with the predominant fracture orientation and fracture trend across the survey area.

Finally, based on the results from the 2D and 3D data sets, an attempt was made to identify undrilled sweet spots in the two areas for which data was available.

SCOPE OF THE STUDY

Production in the Cretaceous Austin Chalk in Central Texas began with the discovery of the Pearsall Field in 1935 (Tyler et al. 1983). Activity in the Austin Chalk increased with the discovery of the Giddings Field in Lee and Burleson counties. The Giddings field in Burleson County is one of the case studies discussed in this paper (Figure 1).

Interest in the Chalk declined with faltering oil prices around 1982, and production depended penetration of natural fractures (Snyder and Craft 1977). Wells drilled at that time were vertical wells and the well data, depths and production, used in the case study are from vertical wells. The boreholes penetrated, and therefore drained relatively few fractures, as the open fractures in the subsurface are vertical. Production wells had short production histories with rapid decline curves (Tyler et al. 1983).

New interest in the Austin Chalk developed with the refinement of horizontal drilling, and by 1996 major operators in the Austin Chalk had drilled more than a thousand new wells into the Chalk. Horizontal drilling penetrates more fractures within the chalk, and provides a better return on investment.

Horizontal drilling has spurred renewed interest in previously exploited areas that were considered depleted or uneconomical. New interest in gas production and more economical and efficient drilling has led to continuing interest in the Austin Chalk, and new areas of exploration and production are now opening up in the Austin Chalk.

Production in the Pearsall and Giddings fields shows the main trend of the Austin Chalk across South Central Texas (Hinds and Berg 1990). Figure 2. The trend is parallel to the strike of the Austin Chalk Formation. It has been estimated that production in the Austin Chalk has amounted to more than 150 million barrels of oil. The oil generated in the Chalk, however, can be calculated in the billions of barrels (Ewing 1983). Much oil is still in place. Current market demand for natural gas has also renewed interest in the Austin Chalk, because it can produce natural gas in economical quantities close to market. Exploration for gas has supplemented oil exploration within the Austin Chalk.

The most important factor for finding successful production within the Austin Chalk is location of zones of abundant natural fractures (sweet spots).
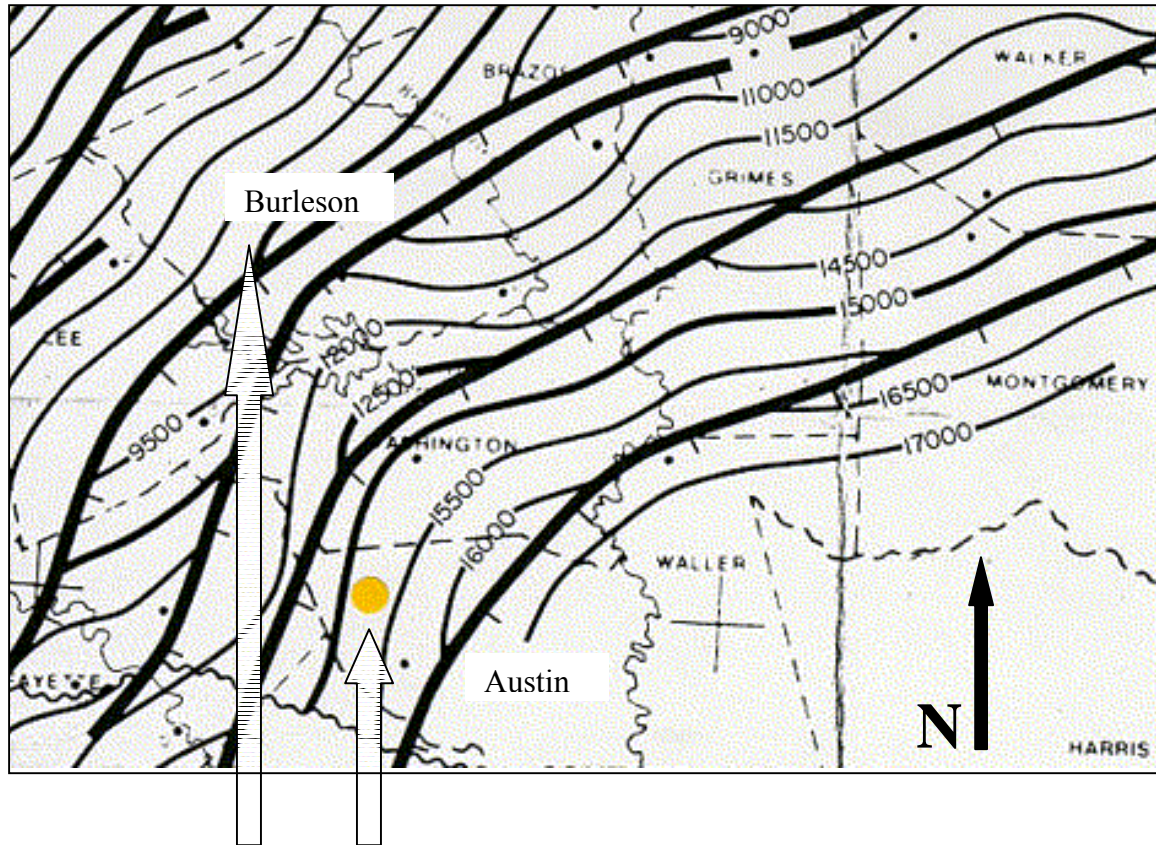
Figure 1. Map of Texas Counties with smoothed contours showing depth to the top of the Austin Chalk (Western Geco). Arrows point to Burleson County and the location of the Walnut Creek area in Austin County. The 2D data set is spread out over most of Burleson County. This figure is shown to show the location of the data areas and the spatial relation between the 2D data in Burleson County and the 3D data in Austin County.
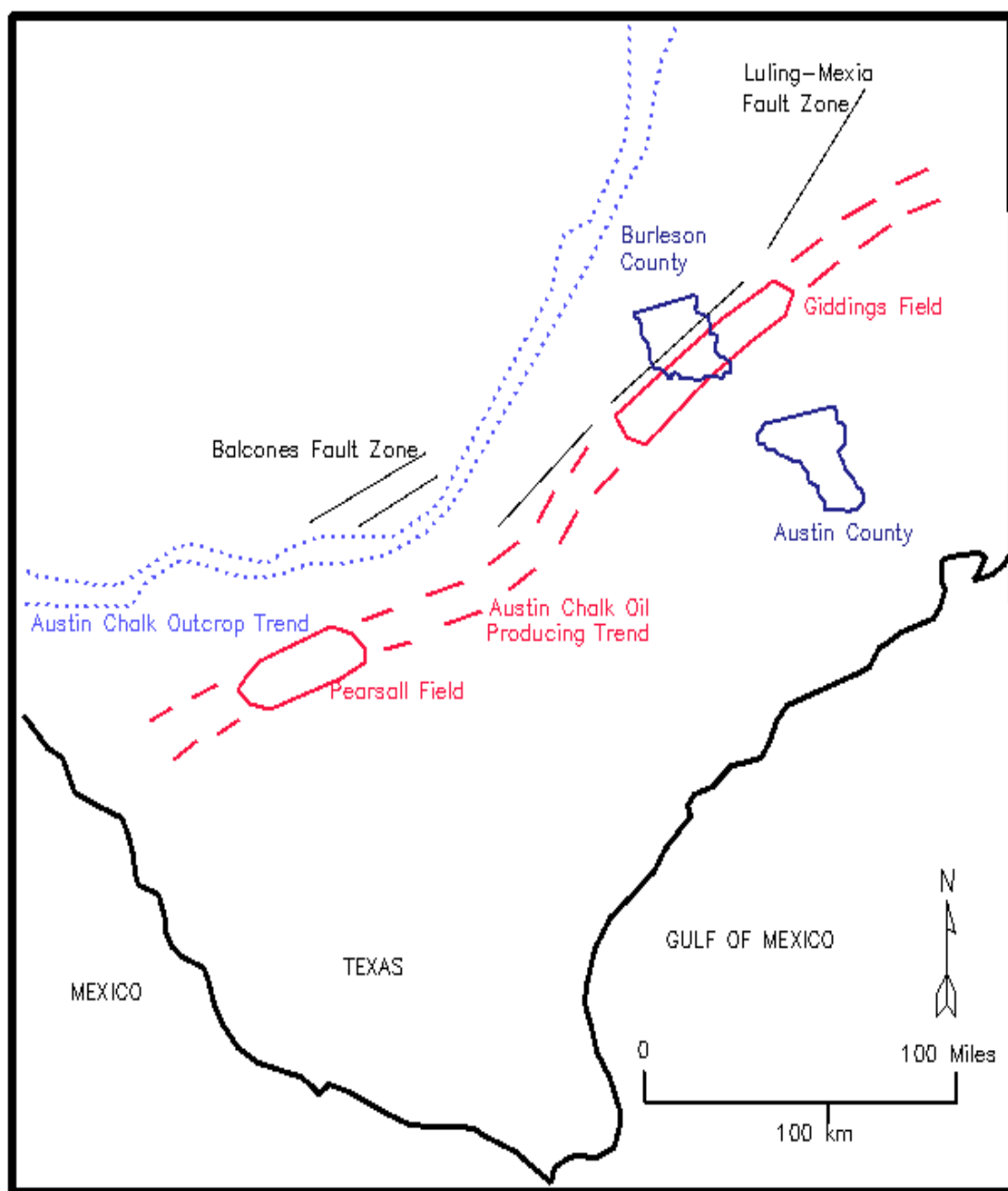
Figure 2. The Austin Chalk outcrop trend with the major oil producing trend including the Pearsall and Giddings fields. The Balcones and the Luling-Mexia fault zones are marked with solid lines.

The problem is to successfully identify these fracture zones and be able to then propose drilling locations. A great deal of 2D seismic and 3D seismic data exist, and new data is being acquired. Identifying fractures with a method that can be applied to existing data would make both existing data as well as new data more valuable.

2D and 3D data used in this study cover areas in Austin and Burleson counties in Texas.

- The Giddings field in Burleson County Texas is extensively covered by 2D data and production data available for this area. I use production data as a proxy indicating fracturing and zones of abundant natural fractures.

- The Walnut Creek area in Austin County Texas is covered by a 3D data set. Three volumes of data were available for the Walnut Creek survey.

  - 1) Regular stack volume with all azimuths;

  - 2) Stack volume with azimuth parallel to strike;

  - 3) Stack volume with azimuth perpendicular to strike.

I have extended my methodology to this area where it indicates a number of prospects.

GEOLOGY OF THE AUSTIN CHALK

The Austin Chalk is a predominantly fine-grained limestone with the majority of grains ranging from 0.5 to 4.0 micrometers (Corbett et al. 1987). The Austin Chalk does contain some coarser skeletal fragments (Cloud 1975). Matrix porosities in the Austin

Chalk range from 1-16% (Cloud 1975). Subsurface porosities at reservoir depths are around 3-4% (Corbett et al. 1987).

The regional dip of the chalk is a gentle dip of approximately 3 degrees to the southeast towards the Gulf of Mexico. The strike of the chalk layer in the subsurface is generally northeast - southwest. The strike and dip trends of the Austin Chalk follow the regional trend in both Burleson and Austin counties.

Production is mainly oil and the width of this oil production trend is approximately 20 miles wide. Oil production depths range from 5000 feet to greater than 10000 feet with the oil generation window from 6000 to 9000 feet (Hinds and Berg 1990). Below the 10000 feet depth the reservoir is mainly gas charged. With production expanding to include natural gas in addition to oil, exploration limits of the Austin Chalk reservoir have extended further to the southwest. The thickness of the Austin Chalk ranges from less than 200 feet to more than 1000 feet. Within the study area the chalk thickness ranges from 200 to 400 feet.

There are two orthogonal fracture sets in outcrops of the Austin Chalk: vertical fractures which are parallel and perpendicular to strike (Friedman et al., 1995, Corbett et al. 1987, Lewallen 1992). The borehole formation evaluation data and production data show that among the two sets of fractures the northeast trending set is open in the

subsurface. The northwest trending set develops only at outcrops (near surface) or is closed off in the subsurface.

Regional stresses are extensional. Major fault zones in the area are the Balcones fault zone, the Luling Mexia and the Talco fault zones. These fault zones are northwest of Burleson County (Figure 2).

The Chalk is underlain by the Eagleford Shale, which is then underlain by the Buda Limestone. The Taylor Marl overlays the Chalk. The Eagleford is a black, limey carbonaceous shale and a probable source rock, but the Chalk section contains sufficient petroliferous shale to be a possible self-sourcing layer (Lewallen 1992) (Figure 3). The Buda and Eagleford are not definable reflectors in the Walnut Creek area and the Edwards is the seismic reflector that underlays the Austin Chalk.

The chalk consists of three lithologic units: A- an upper brittle chalk unit, B- a ductile unit and C- a lower brittle unit. The upper unit A may not be present in the entire Chalk trend. The oil generated in this layer of the Chalk is estimated to be in the billions of barrels (Ewing 1983). The brittle lower unit C and to some extent the upper unit A contain more abundant fractures. Therefore they are the main producing zones. The middle unit B is relatively less fractured and not a good reservoir. The three units of the Chalk can be identified in well logs, such as gamma ray (GR).

TERTIARY	PALEOCENCE	WILCOX	●
		MIDWAY	●
CRETACEOUS	GULFIAN	NAVARRO	●
		TAYLOR	●
		AUSTIN — A	●
		AUSTIN — B	
		AUSTIN — C	●
		EAGLEFORD	
		WOODBINE	
	COMANCHEAN	BUDA	●
		DEL RIO	
		GEORGETOWN	●
		EDWARDS	●

Figure 3. Generalized stratigraphy of the Giddings Field area. The Austin Chalk is divided into three layers A, B and C. Productive intervals are marked by black dots (Hinds and Berg, 1990).

Formation micro-scanner (FMI) logs are required to identify fractures in the boreholes. These logs are expensive and are not available in the boreholes used in this study in Burleson County. The GR response within the Chalk has lower values than the Taylor marl above and the Eagleford shale below. The spontaneous potential (SP) log response also has a lower value within the Chalk compared to the layers above and below (Figure 4). Within the Austin Chalk, the units can be separated by the log response. The GR response for the top unit A and lower unit C indicates very little shale content within the chalk. The middle unit B can be distinguished by the increase in shale content as seen by the increased response in the gamma ray curve (Figure 4).

A dip section from the Walnut Creek survey is shown in Figure 5. The top of the Chalk (TOC) and the base of Chalk (BOC) is marked on the section. Several faults are interpreted along this section. The interesting feature is that the prominent fault deeper in the section does not penetrate the Chalk. The fault forms a shelf edge that influences overlying structure. The Chalk is under extension where it is draped over this fault. This is a good area to find open fractures within the Chalk. The faults are extensional normal faults on either side of this edge. They do not have a lot of vertical displacement and the faults do not seem to extend further into the seismic section above or below the Chalk. Reduction in amplitudes associated with the faults is evident on this section.
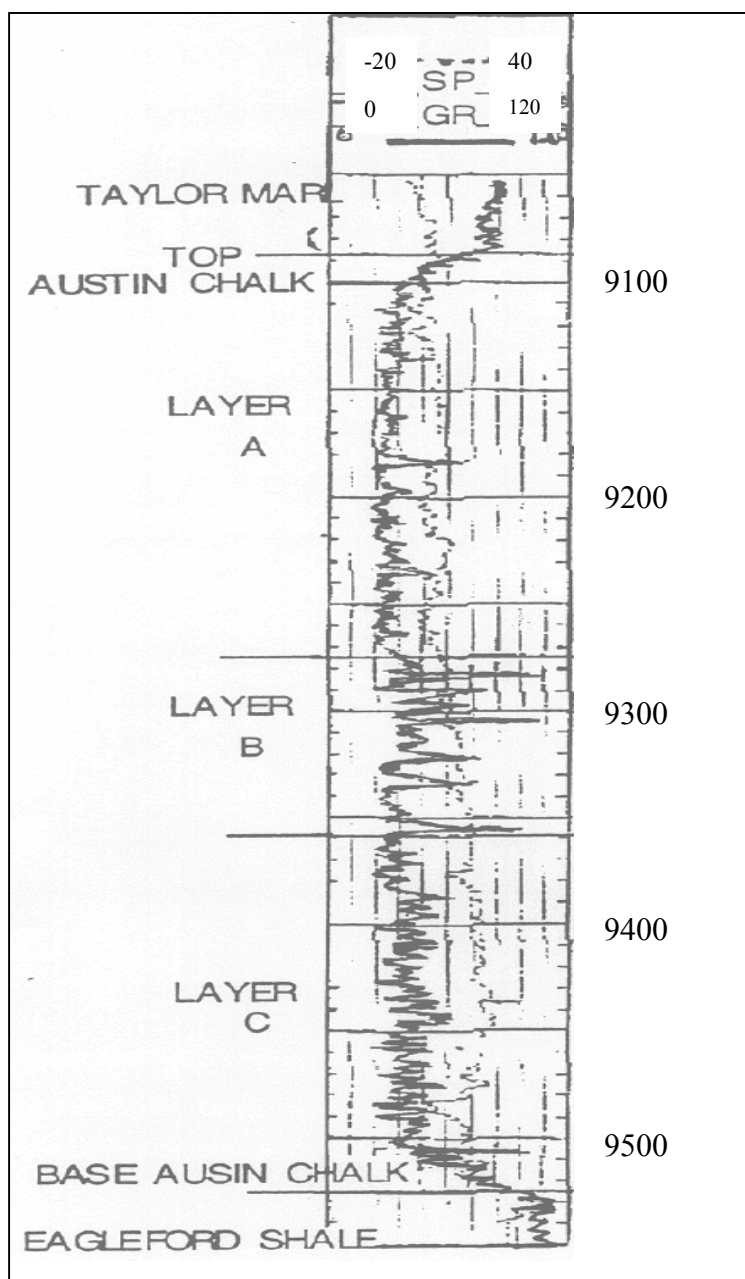
Figure 4. Individual Chalk layers marked on a well log section from Burleson County (Corbett 1982). A decrease in gamma ray response indicates the Top Austin Chalk. All Austin Chalk layers A, B and C are characterized by low gamma ray response. However, Layer B has a different gamma ray response character, in comparison to layers A and C, due to interspersed shale.

Figure 5. A dip line from the Walnut Creek survey. The top of the chalk (TOC) and the base of the Chalk (BOC) are both marked on the section. Several faults (white lines) are interpreted along the section, and the reduction in amplitudes associated with the faults is evident on this section.

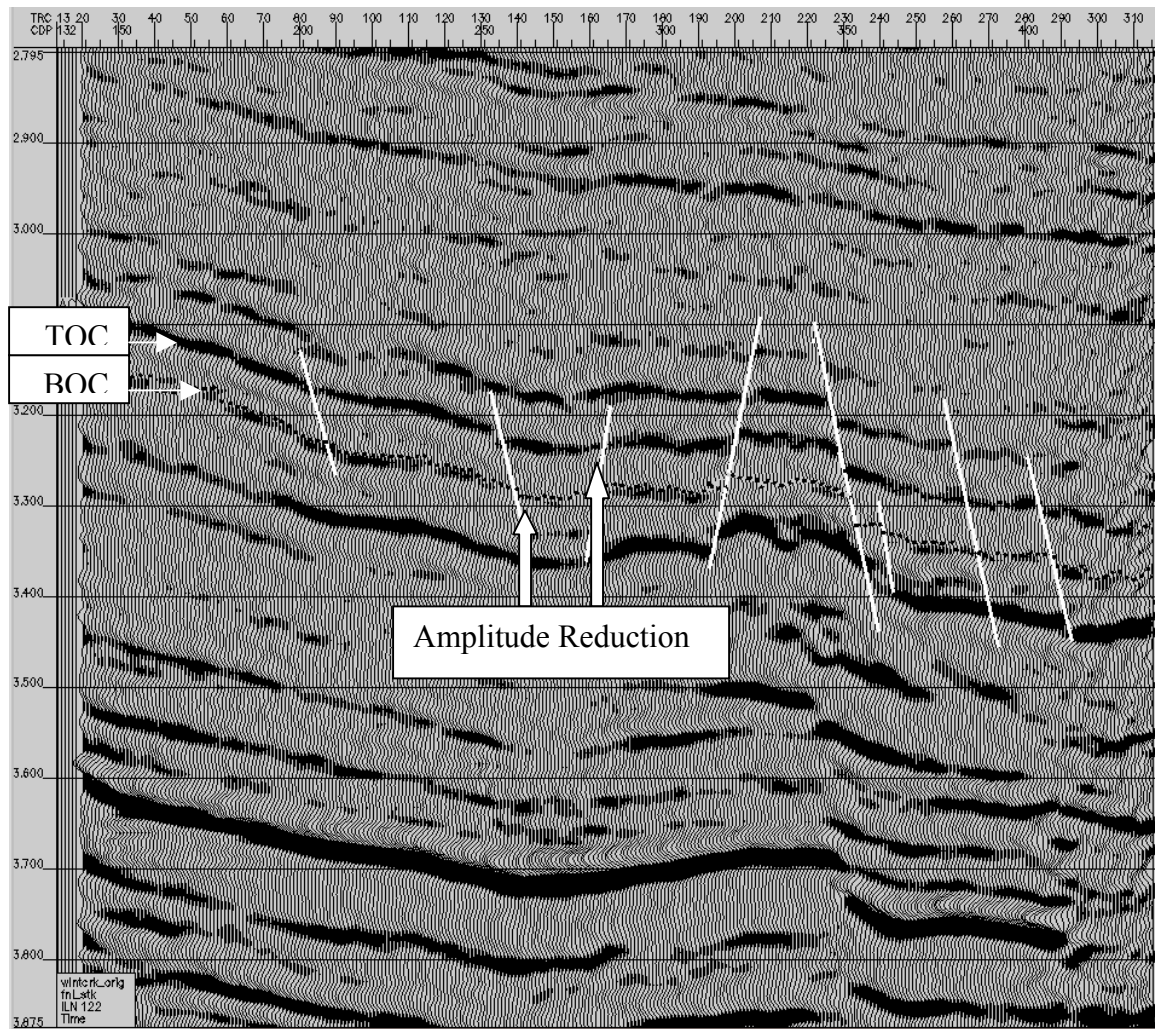A 2D seismic section from Burleson County is displayed in Figure 6. Faults (F) are interpreted along with the Top of Austin Chalk (TOC) and Base Austin Chalk (BOC) reflector. A reflection magnitude section of the same line is displayed to show the reduction in amplitudes associated with faulting. The faults do not have a lot of vertical displacement. Wells with production are projected onto the 2D line. These wells are close to interpreted faults.

Seismic data does not show fracture signatures directly. Seismic attributes used in the detection of fractures include AVO signatures (Al Shuhail 1998), S-Wave attenuation and anisotropy (Crampin et al. 1989, Al-Mustafa 1992) and amplitudes attenuation due to absorption and scattering (Hudson, 1981, 1988; Richards and Menke 1983). Other techniques such as cross-hole tomography and VSP methods have been used but require borehole seismic data. These methods are limited, by extent of coverage, expense and availability and are not discussed further in this study.

I use spectral shifts in 2D and 3D seismic data to develop a fracture detection technique. This technique will be discussed in detail below.

Fracturing has a close correlation with faults in the Austin Chalk. There has been production from both the up-thrown and down-thrown blocks in the proximity of faults. (Hinds and Berg, 1990). A correlation between the frequency attenuation and amplitude anomalies associated with faults is discussed in chapter 4.
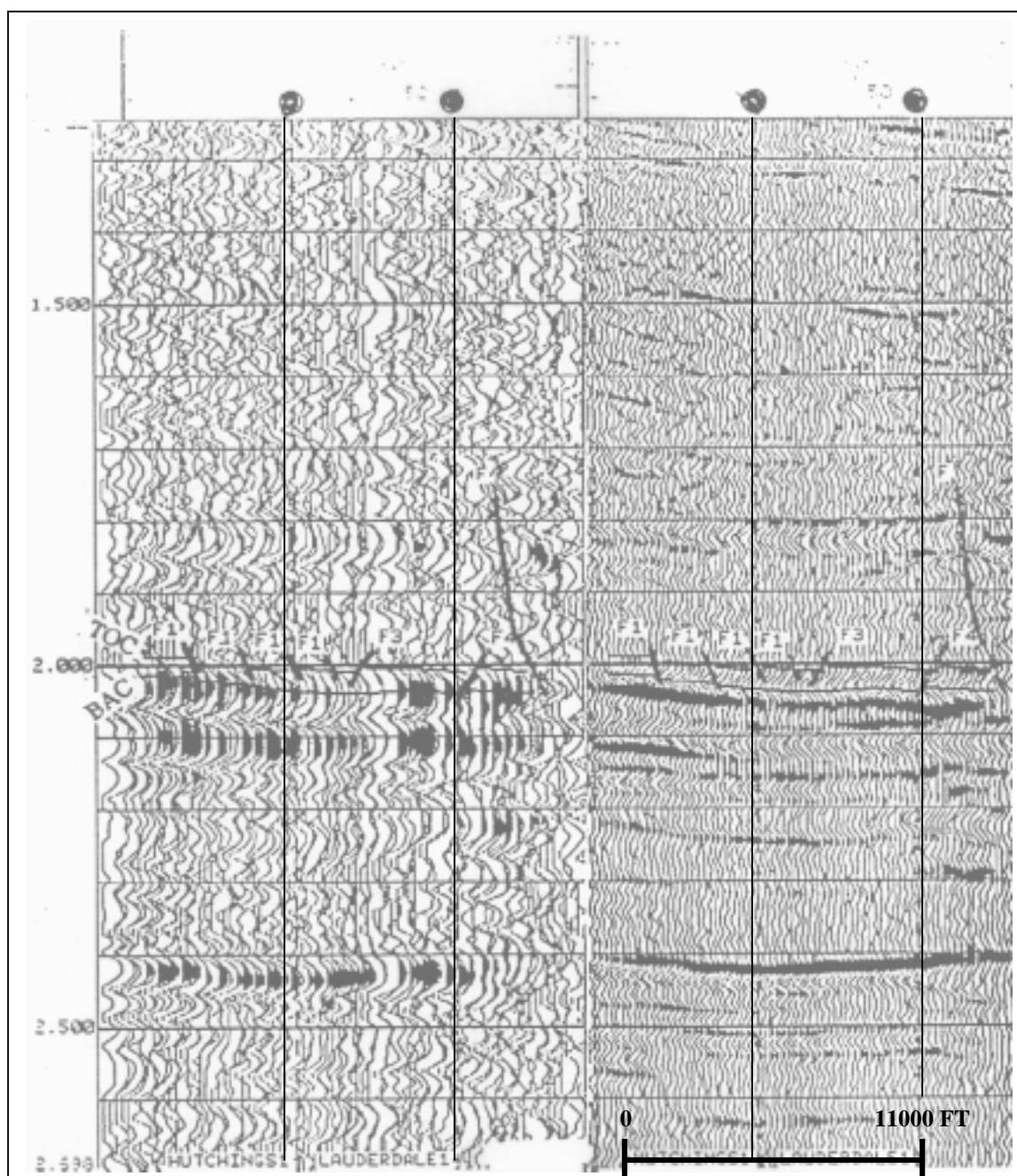
Figure 6. 2D dip line CAGB15. Faults (F) are interpreted along with the Top of Austin Chalk (TOC) and Base Austin Chalk (BOC) reflector. A reflection magnitude section (left) displayed illustrates the reduction in amplitudes associated with faults. Production wells are displayed on the section.

3D DATA

 The data set used for this study is a 3D seismic survey with inlines oriented N50W -

S50E. These inlines are parallel to the dip direction of the Austin Chalk layer. The

inline spacing is 440 feet with the CDP spacing of 110 ft. TOC in this survey ranges

from 3000 to 3500 milliseconds with a regional dip to the southeast (Figure 7). The

coverage is at an average 24 fold for the entire data set.

This initial data set was used to separate out strike and dip azimuths based on shot

receiver geometry. For example, the shot/receiver azimuths accepted for the dip

orientation was + or - 20 degrees from the dip orientation of S55E. (Figure 8)

Two additional volumes were derived from the original to give a total of three data sets.

1. The original 3D data set.

2. Dip azimuth 3D data set (stacked data of traces limited within orientations + or
   - 20 degrees from the regional dip orientation of N55W-S55E).

3. Strike azimuth 3D data set (stacked data of traces limited within orientations +
   or - 20 degrees from the regional strike orientation of N35E - S35W).
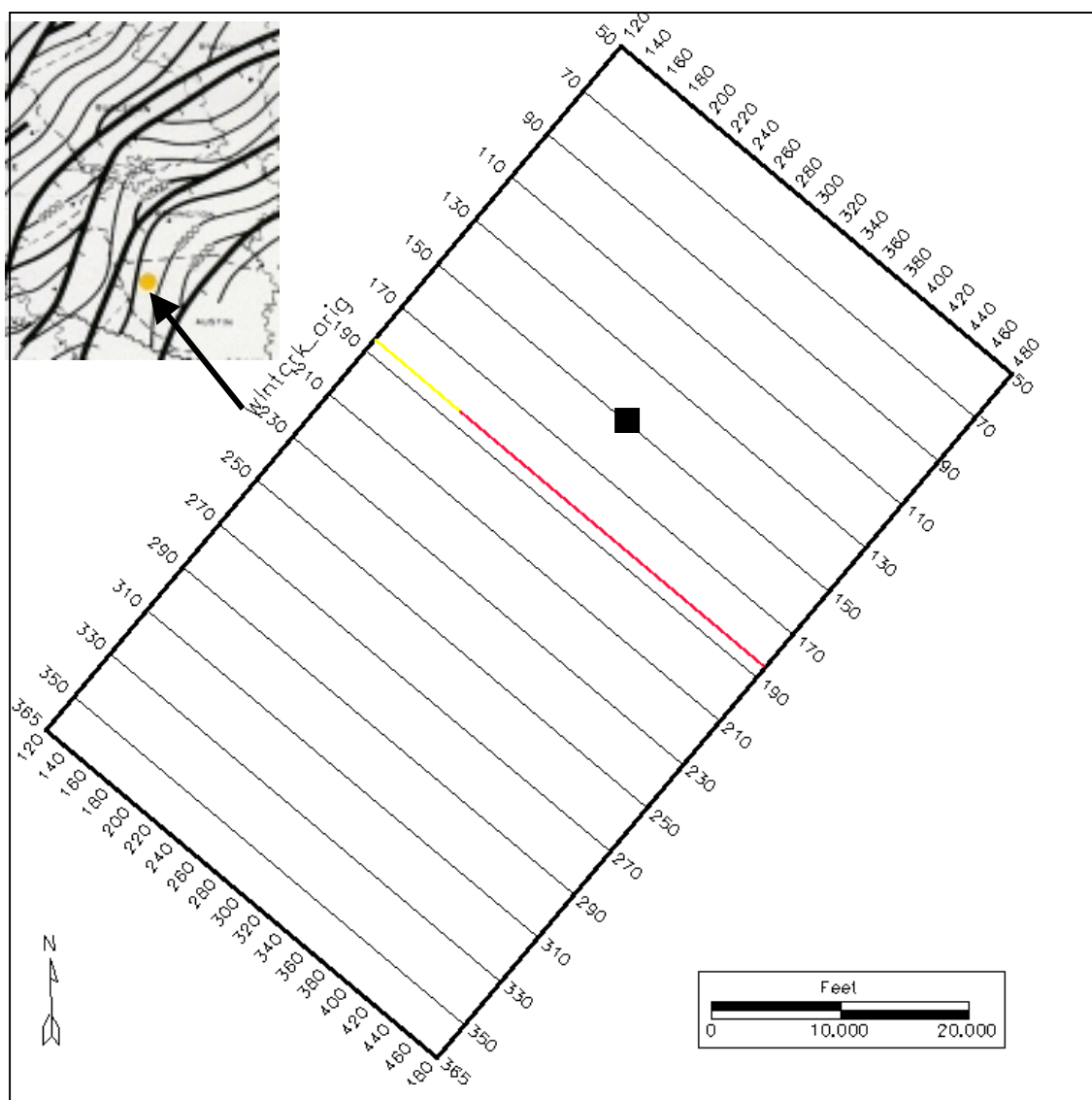
Figure 7. Walnut Creek Data set survey map. The lines are oriented northeast -

southwest. Line spacing is 220 feet. Crossline spacing is 110 feet. Line150 - CDP300 is

marked with a black square to show the location of the trace used for sample spectra

data. The inset shows location of the survey in Austin County.
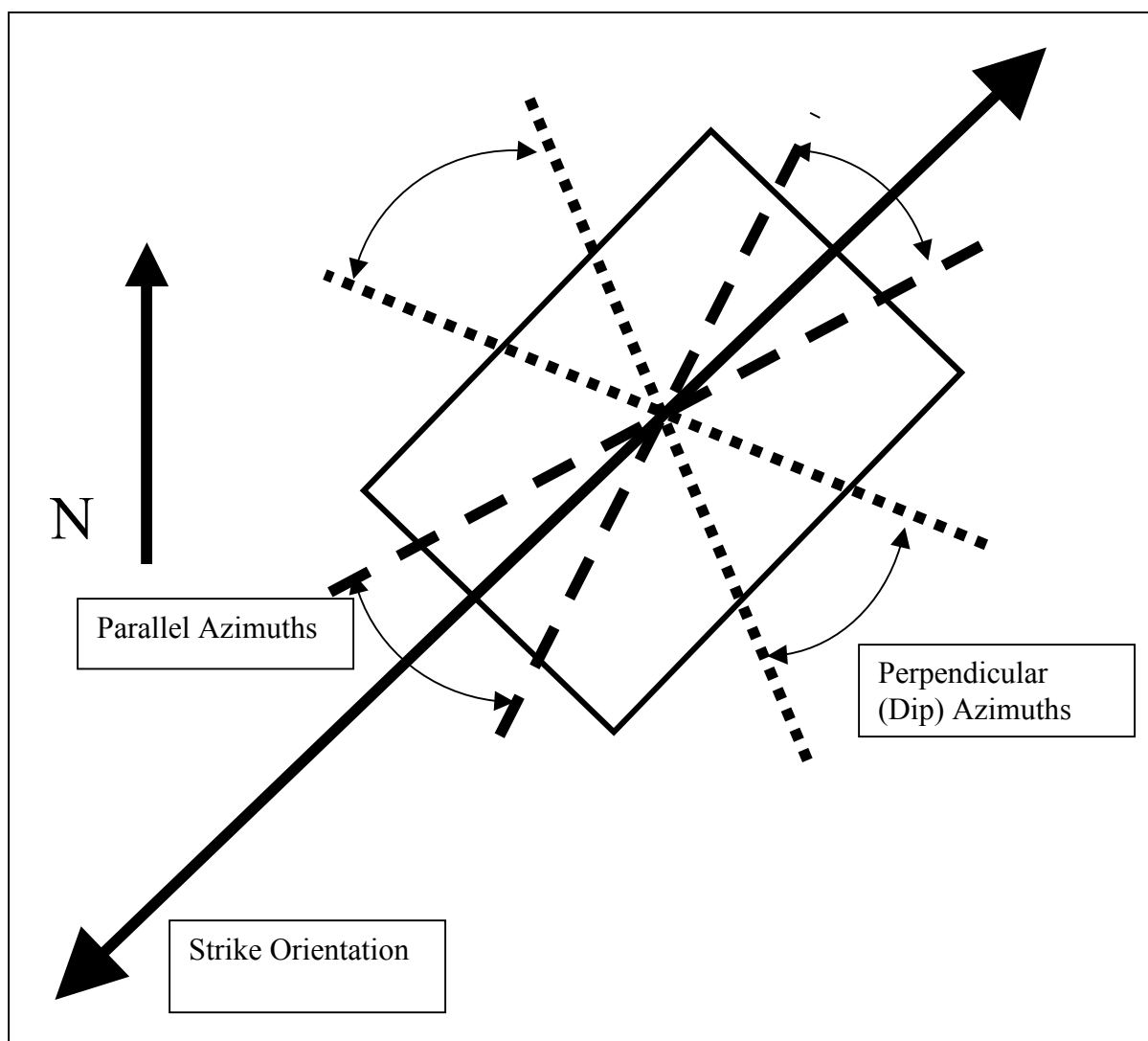
Figure 8. Illustration showing how azimuths were taken for the two additional data sets

derived from the initial 3D data. This is based on Shot – CDP orientation of the survey

given in Figure 7. The solid arrow gives cross line and the strike orientation. The

dashed arrows are subparallel to strike (+ or - 25 degrees) and give the range of

orientations of the parallel (to strike) azimuth data set. The dotted arrows are

subparallel to dip and give the range of azimuths taken for the perpendicular azimuth

data set (perpendicular to the strike).

2D DATA

The 2D data is a set of dip lines that do not form a regular grid and only a few lines are in the strike orientation (Figure 9).

The data set consists of 70 2D lines that cover approximately 150 line miles. The seismic data is within the area where the chalk is at depths of 6000 to 10000 feet. These depths are within the oil generation window for the Austin Chalk formation (Hinds and Berg 1990). The lines are predominantly dip lines and do not form a regular grid, as seen in Figure 9. Time interpretation for the top of the Austin Chalk layer in Burleson County gives a regional dip to the southeast. Reflection magnitude data was extracted on the interpreted chalk horizon. The vertical displacements on the faults interpreted were generally less than 10 ms. Faults were interpreted on individual lines. However, the faults could not be correlated from line to line with any confidence. The following points briefly describe the quality and the processing of the seismic data.

The average stack of the seismic data is 10 fold.

Dip Move Out correction was applied to the data during processing.

No additional migration was applied during processing.
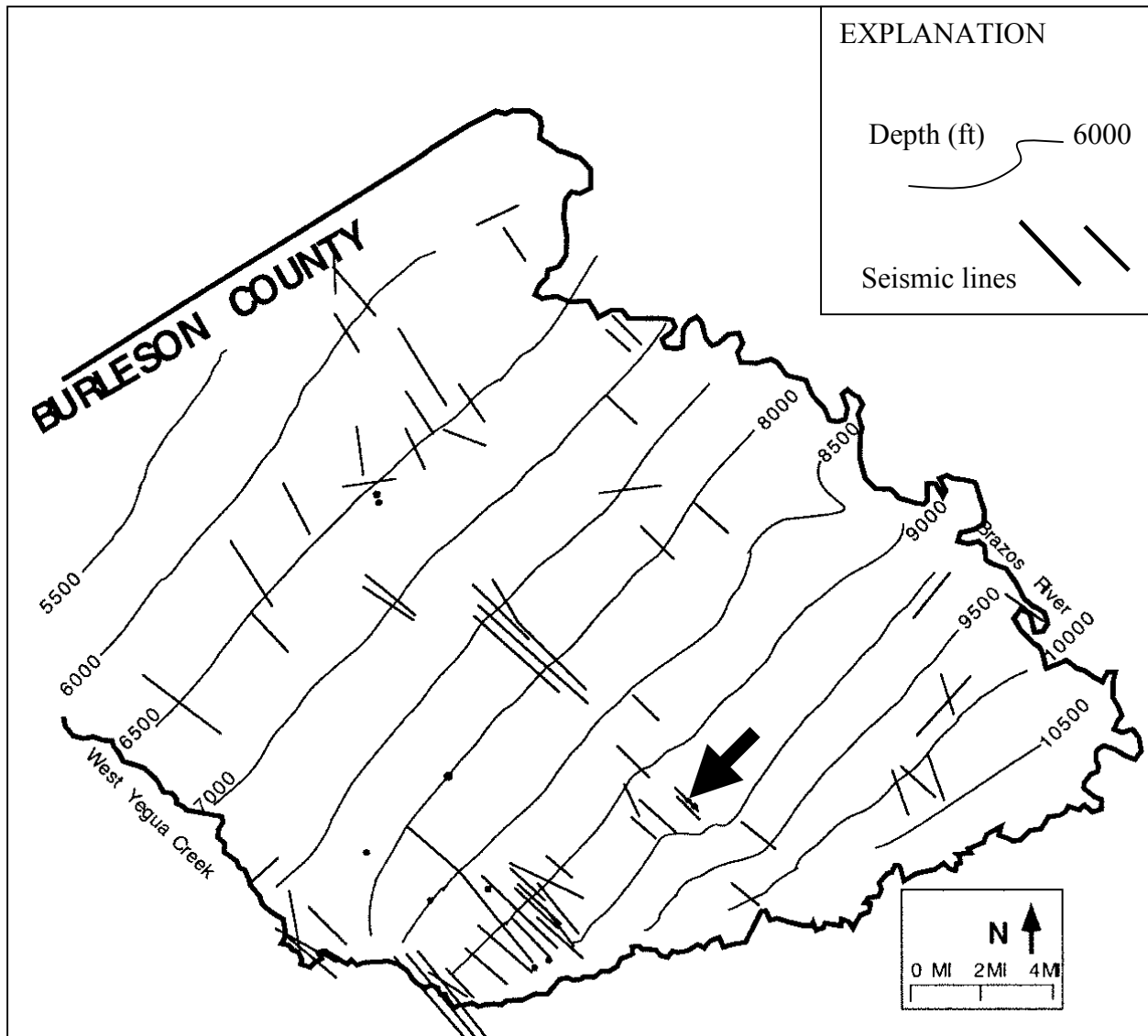
Figure 9. Burleson County 2D data represented as line locations. The depth contours plotted on the map are based on well data. Well locations are shown as solid dots. The majority of the 2D lines cross the contours at right angles (dip lines). The 2D data do not form a regular grid of intersecting lines. The 2D line used for examples in Figure 6, 10 and 11 is marked with an arrow.

FREQUENCY DEPENDENT ATTENUATION OF AMPLITUDES:

A FRACTURE INDICATOR

't*'

The attenuation of frequency due to fracturing is presented as a fracture indicator in this paper. Haugen and Schoenberg (2000) discuss the effect of scattering by fractures and the dependence or relation between scattering and wavelength. Schoenberg (1988) discusses the preferential attenuation of higher frequency amplitudes from seismic data. Liu et al. (1997) and Gibson et al. (2000) discuss the diffraction of fracturing using synthetic data derived from theoretical and physical models. The attenuation by scattering is sensitive to both fracture size and shape. Chalk attenuates higher frequencies preferentially due to scattering and absorption (McCann and McCann 1985 and Guigne et al. 1989). Therefore the main mechanism for attenuation appears to be scattering and/or diffraction from fracture edge.

My method is based on the preferential attenuation of higher frequency amplitudes from seismic energy by fracturing. The comparison of frequency spectra from seismic time windows above and below the Chalk shows a shift in spectra towards lower frequencies. Frequency spectra are derived for every trace from over these two time windows.

A fracture indicator is developed based on frequency amplitudes from the seismic data. Amplitude values at specific frequencies are taken from the spectra and used in the equation derived below. The equation gives an attribute value, which is called t*. The t* attribute are related to the amplitude attenuation of frequencies due to fractures. Higher t* values indicate:

- Higher fracture density

- Larger thickness of the layer is fractured,

- Or a combination of the two

The fracture indicator gives a qualitative attribute to indicate fractures (sweet spots) on seismic data. It does not give a quantitative measure of the amount of fracturing.

PROCEDURE

The data used is P-Wave reflection data from the data sets described above.

The data is windowed by a 100-millisecond time window immediately above the interpreted Chalk reflector and a second window 100 milliseconds below the first window. The reason for this window length is to take a sufficient length of the trace to include several reflection events from the seismic section (Figure 9). Attenuation due to geometrical spreading is limited by limiting the time window (Figure 10). Geometrical spreading does not contribute a significant amount of attenuation in this small time window. Time depths are 2000 ms. The frequency spectra are derived for each trace for both time windows (Figure 11) from above and below the Austin Chalk. Frequency spectra of seismic traces from 100ms window above the Chalk are compared with spectra from the 100 ms window below the Chalk.
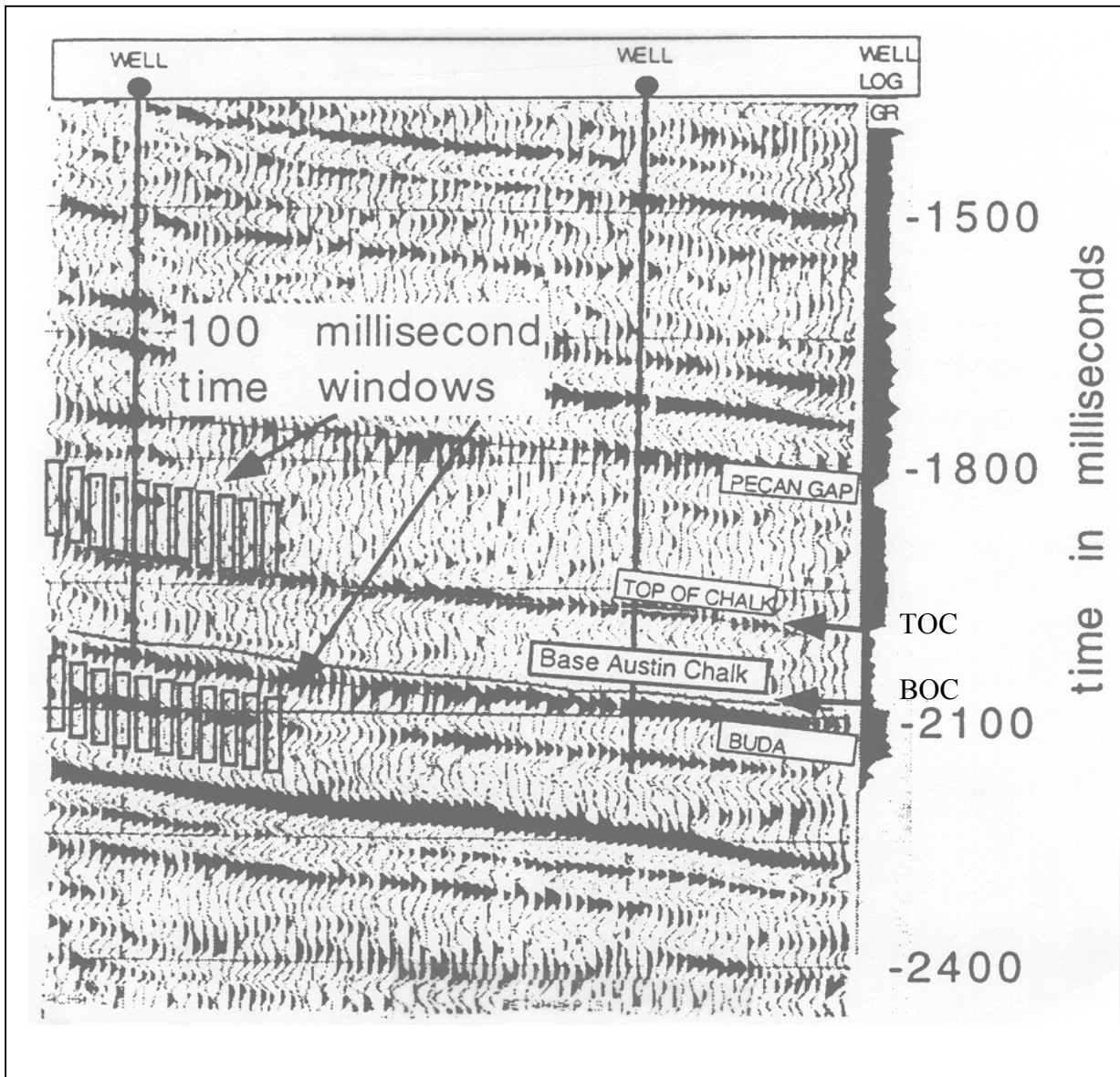
Figure 10. Seismic section of the 2D line CAGB15 is displayed. TOC and BOC were determined from the gamma ray log. 100 ms time windows are marked on the section to illustrate the time windows used above and below the chalk. Trace data within these windows are used to extract the frequency spectra.
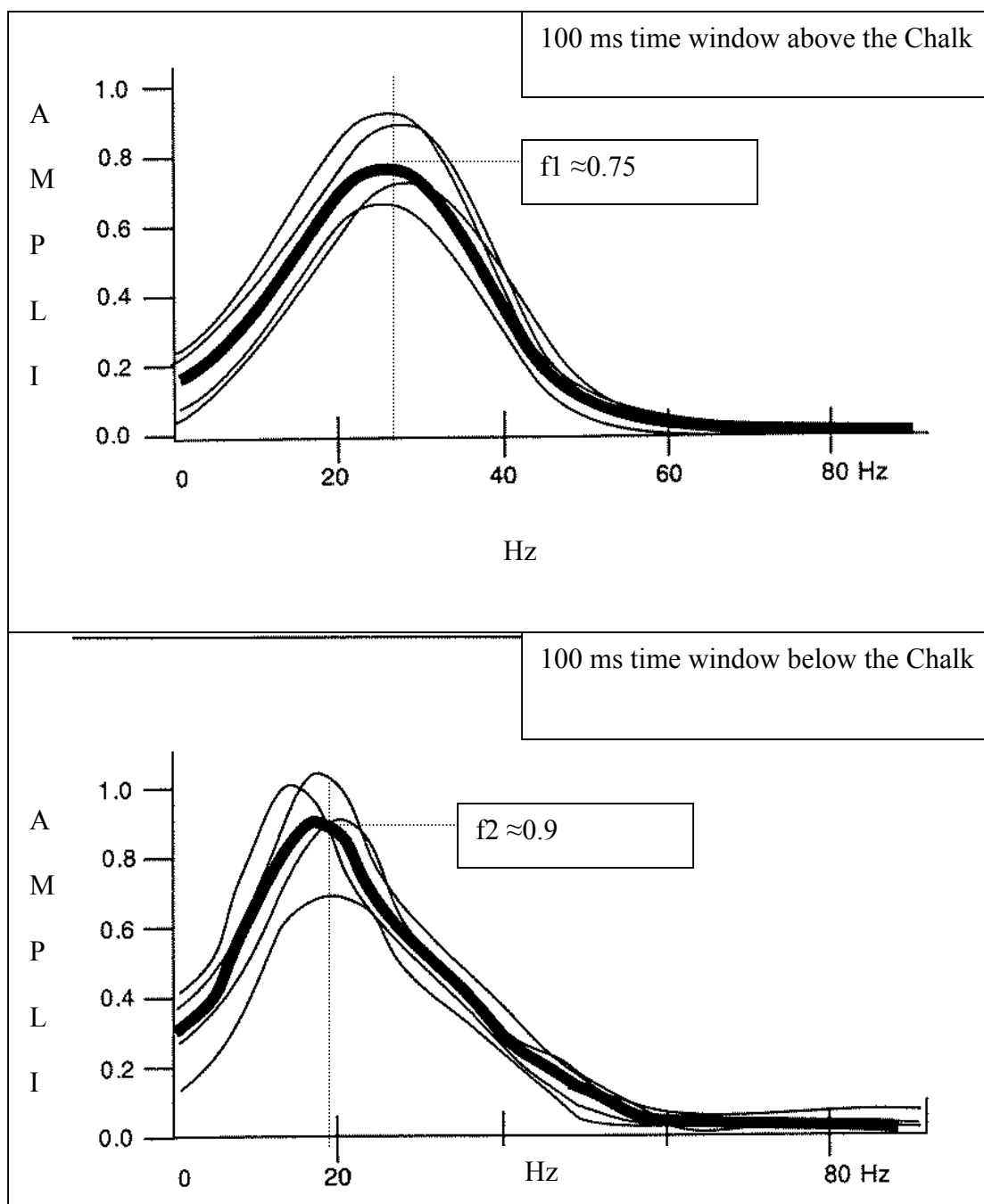
Figure 11. Normalized frequency spectra from four traces of the 2D line indicated in Figure 10 showing a 10Hz shift in peak amplitude in upper and lower windows. The heavy curve represents the average.

The spectra were calculated using cosines correlation method developed

(Geoquest/Schlumberger) to be interactive with Geoquest's seismic interpretation

software. There was no bandpass filtering applied in calculating the spectra.

The shift in peak frequency towards the lower frequencies illustrates the attenuation of

higher frequencies (Figure 11). Frequency amplitudes at 10 Hz (f1) and 30 Hz (f2) from

above the Austin Chalk (A1) and from below the Austin Chalk (A2) are extracted from

the frequency spectra for each trace. A qualitative number is derived using these

frequency spectra ratios using the method described below (Najmuddin 2001):

Derivation:

Carmichael (1990) gives the equation

$$A(f,X) = G \times S(f) \times R(f) \times \exp(-\alpha\, X\, f)$$

G - Geometrical Spreading; S(f) - Source function; R(f) - Receiver function

Substituting $t^* = -\alpha\, X$

$$A1(f,X) = G \times S(f) \times R(f) \times \exp(f\, t^*1)$$

For a specific travel time (fixed distance):

$A1(f,X) = G \times S1(f) \times R1(f) \times \exp(f\, t^*1)$ (Represents time window above the Chalk)

$A2(f,X) = G \times S2(f) \times R2(f) \times \exp(f\, t^*2)$ (Represents time window below the Chalk)

$$\ln(A1) = \ln(G) + \ln R(f) + \ln S(f) + (t^*1)f$$

$$\ln(A2) = \ln(G) + \ln R(f) + \ln S(f) + (t^*2)f$$

$$\ln(A1/A2) = \ln(G/G) + \ln(R(f)/R(f)) + \ln(S(f)/S(f)) + (t^*2 - t^*1)f$$

The total time window is limited to 200 ms, therefore the difference in the geometrical spreading term G is assumed to be negligible and it cancels out.

The source and receiver terms are the same for the same trace and they also cancel out. This leaves:

$$\ln(A1/A2) = (t*2 - t*1)f$$

Amplitudes of the frequency spectra are taken at two specific frequencies f1 and f2.

$$\ln(A1/A2)(\text{at } f1) = (t*2 - t*1)f1$$

$$\ln(A1/A2)(\text{at } f2) = (t*2 - t*1)f2$$

$$\ln(A1/A2)(\text{at } f2) - \ln(A1/A2)(\text{at } f1) = (t*2 - t*1)(f2 - f1)$$

or

$$t* = (t*2 - t*1) = [\ln(A1/A2)(\text{at } f2) - \ln(A1/A2)(\text{at } f1)] / (f2 - f1)$$

DISCUSSION OF NOISE IN THE DATA

Spherical divergence correction was applied to the data during the processing sequence. Spherical divergence correction increases the gain of the noise along with the signal. The frequency content of the traces is significantly affected by the noise present in the data. There may be some attenuation of frequencies due to reasons not related to fracturing, and there may be some attenuation of frequencies due to other layers above the Chalk. These factors cannot be quantified or corrected for. Therefore there may be some error in the t* value due to noise.

DISCUSSION OF t* ATTRIBUTE VALUES (FRACTURE INDICATOR)

The calculations were done with 2D data and with the three volumes of the 3D data. If the amplitudes spectra are unchanged over an interface the values for t* would be zero. Attenuation of amplitudes at higher frequencies and the shift of the amplitude spectrum towards lower frequencies would give higher values for t*.

Variations in the amplitude spectra are affected by the noise in the data as well as interference, multiples etc. This results in both positive and negative values for t*. Ideally, for a zone not affected by preferential attenuation of higher frequency amplitudes the t* attribute would be zeros. Test values computed for a window, 500 ms above the chalk, range between: –0.52 and 0.33; mean = -0.07. This value is indicative of essentially no attenuation. (Table 1)

Table 1 Statistical representation of t* attribute values.

	Mean	Standard Deviation	Variance	t* val Min	t* val Max
t* Austin Chalk	0.93	1.38	1.92	-5.87	7.89
t* 500 ms above chalk	-0.07	0.09	0.01	-0.52	0.33

The values calculated for the Austin Chalk layer t* range between –5.87 to +7.89. Comparing the layer above the chalk to the Austin Chalk layer there is a marked difference in the range of values (values are an order of magnitude higher). There is

marked shift of the entire distribution towards the positive values with Mean = 0.93 (Figure 12). Higher values correspond to greater frequency attenuation and therefore indicate fractures. Fracture zones are interpreted using the t* attribute as a fracture indicator. This is demonstrated in the case studies for the 2D and 3D data sets.
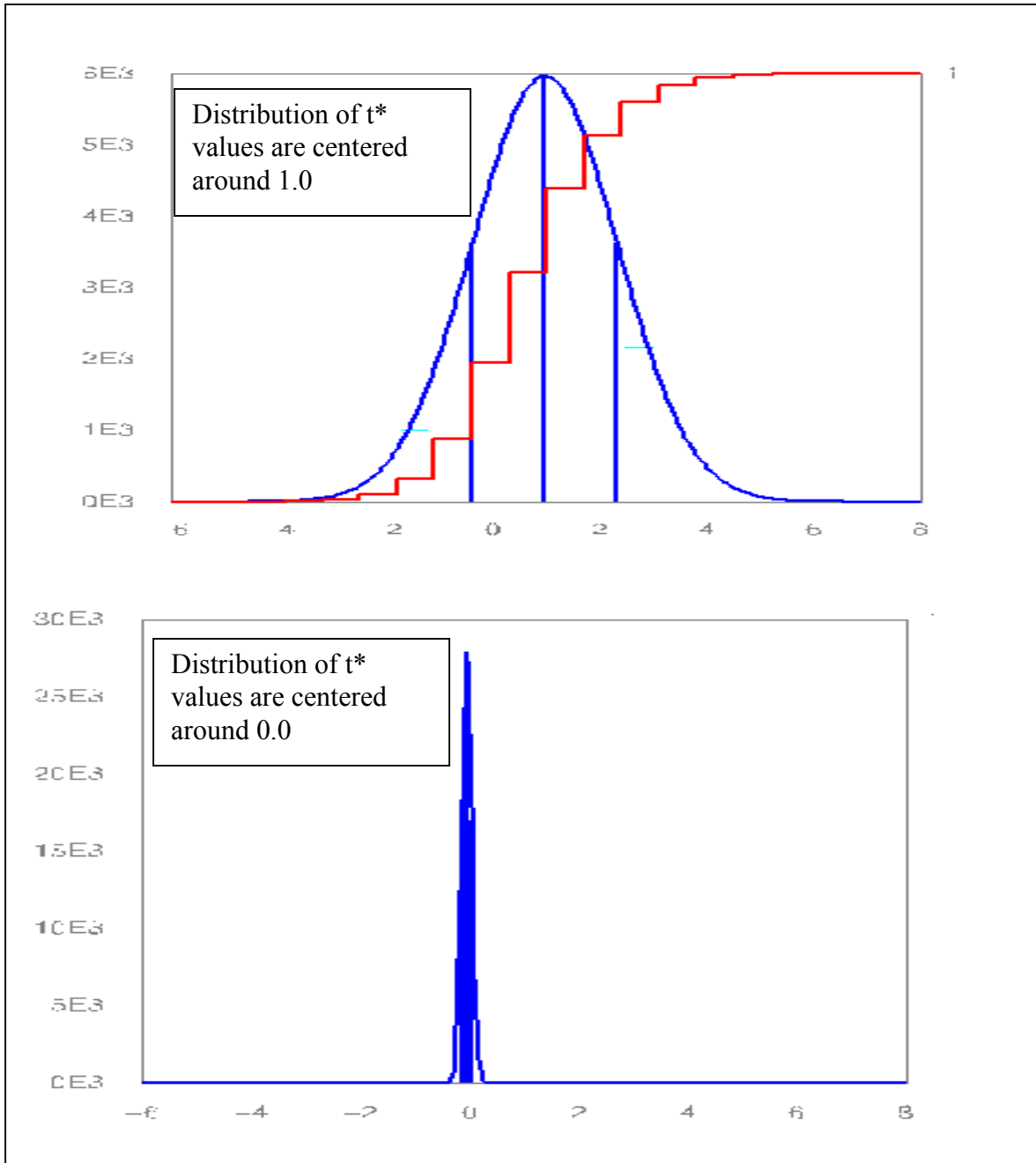
Figure 12. Statistical representation of the t* values derived from the Austin Chalk layer (top) and from the reference layer at 500ms (bottom). The Y axis represents number of samples. The X axis represents the t* values. The center vertical line inside the distribution curve is the Mean value straddled by the standard deviation value lines.

CASE STUDY: 2D DATA SET BURLESON COUNTY

(GIDDINGS FIELD)

Depth to the chalk layers ranges from 5500 feet in the northwest part of Burleson County to greater than 10500 feet to the southeast. Depth contours interpreted from well marker data are shown in Figure 10. The regional dip is approximately 3 degrees to the southeast over this area.

PRODUCTION DATA

Production data from over a hundred wells was used to generate the production map of cumulative production till 1982 (R. Berg personal communication 1995). Cumulative production data was plotted and contoured to give Figure 13. The tops from these wells give the depth data in Figure 10. The wells are distributed across study area, interspersed between the 2D data. The majority of the wells are concentrated within the Giddings Field producing trend.

Production in the Austin Chalk (Figure 13) corresponds to the wells penetrating fracture zones (sweet spots). Therefore, the cumulative production data is a proxy for fracturing.

FREQUENCY DATA

Frequency spectra were generated for every trace from two time windows:

1) A 100 ms window above the top of the chalk layer.

2) A 100 ms window below the base of the chalk layer.

Two values were taken from each spectrum:

- The amplitude value of the spectrum at 10hz

- The amplitude value of the spectrum at 30hz

These were the values used to calculate the fracture indicator attribute t* for each trace.

Figure 11 has several spectra for 100 ms windows both above and below the chalk.

INTERPRETATION OF THE t* ATTRIBUTE VALUES FROM 2D DATA

The t* attribute was mapped over the study area. Fracture zones were interpreted based

on high t* values and then marked on the 2D lines. After marking these zones, the

fracture zones were correlated from line to line on the map (Figure 13). This correlation

was influenced by the assumption of fractures parallel to strike.

The cumulative production data is plotted on the same map to correlate this with the

fracture indicator t* data derived from the frequency spectra. The production data has a

good match with the fracture interpreted from the t* data (Figure 14). There are,

however, several 2D lines to the northwest that have fracture zones interpreted from the

t* data, but do not have production. A possible explanation for this is that these lines

are above the zone of hydrocarbon maturity. There may be migrated hydrocarbons in

these fractures, therefore, there is a possibility of finding oil in these fractures as areas

bypassed or overlooked, with the possibility of finding gas or no hydrocarbons at all.

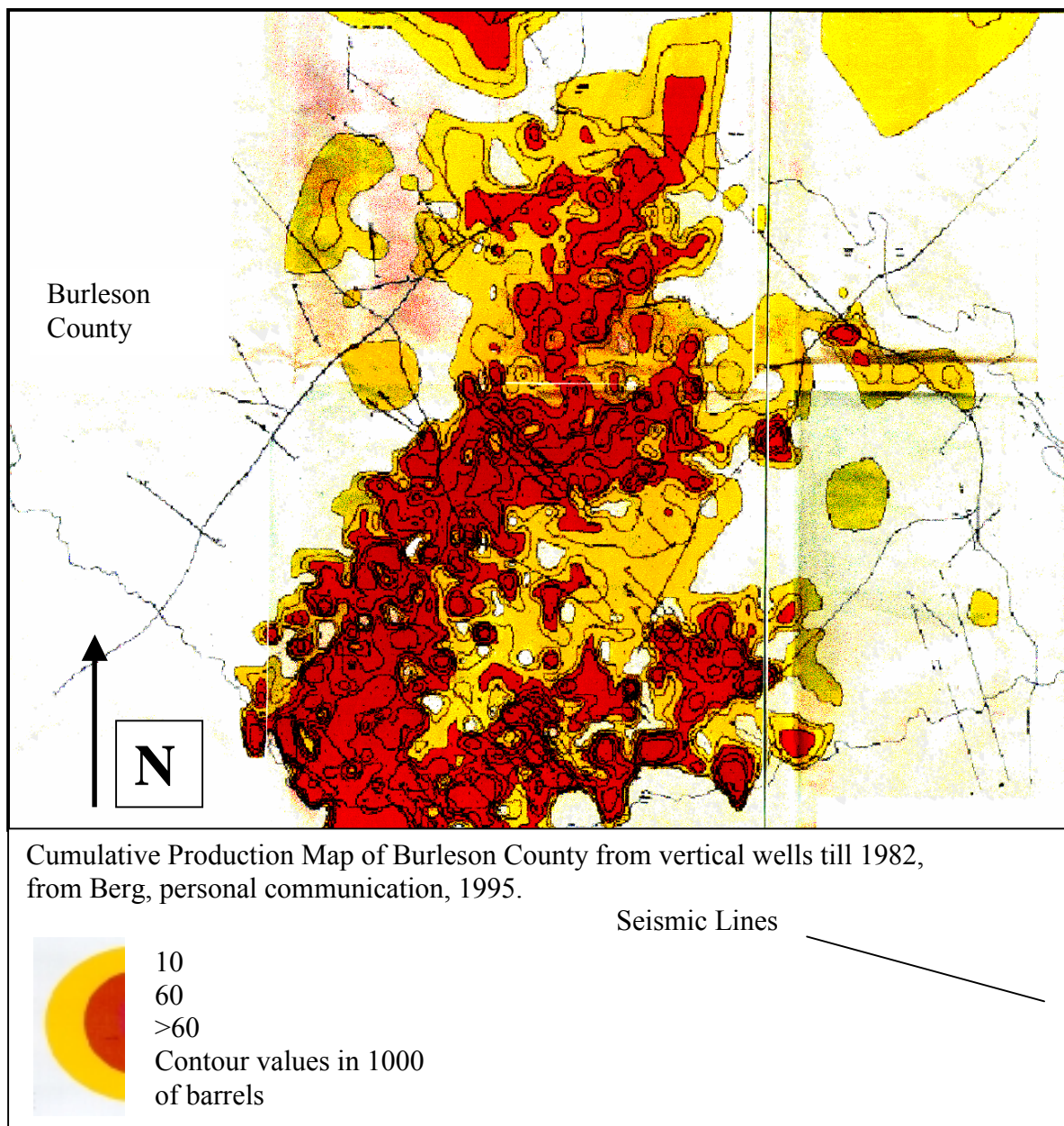Cumulative Production Map of Burleson County from vertical wells till 1982, from Berg, personal communication, 1995.

Figure 13. Cumulative production map of Burleson County (R. Berg, 1995)from vertical wells (production until 1982). The production is shown as colorfilled contours to emphasize the production trend through the area. The production trend is northeast - southwest.

AMPLITUDE ATTENUATION

Scattering and absorption of the seismic energy by fractures affect the reflection magnitude. Therefore amplitude data is another attribute that can be used as a fracture indicator for a known fractured reflector. Decreases in amplitudes are interpreted as fracture zones and are plotted on the 2D lines in the study area (Figure 15). These amplitude anomalies correlate well with the fracture indicator t* attribute.

CONCLUSIONS FROM THE 2D DATA SET IN BURLESON COUNTY

- t* anomalies are consistent with areas of highest production data. This tends to validate t* as a fracture indicator.
- Amplitude anomalies also tend to validate t* as a fracture indicator.
- Fractures zones in the northwest part of the study area, as indicated by the t* attribute, do not correlate with production. This may be due to the area being above the oil maturation window (Hinds and Berg 1990) of 6000 feet. These areas do not fall within the cumulative production trend because they may not have hydrocarbons in economic quantities or may be bypassed if it only had gas shows when the production focus was for oil.

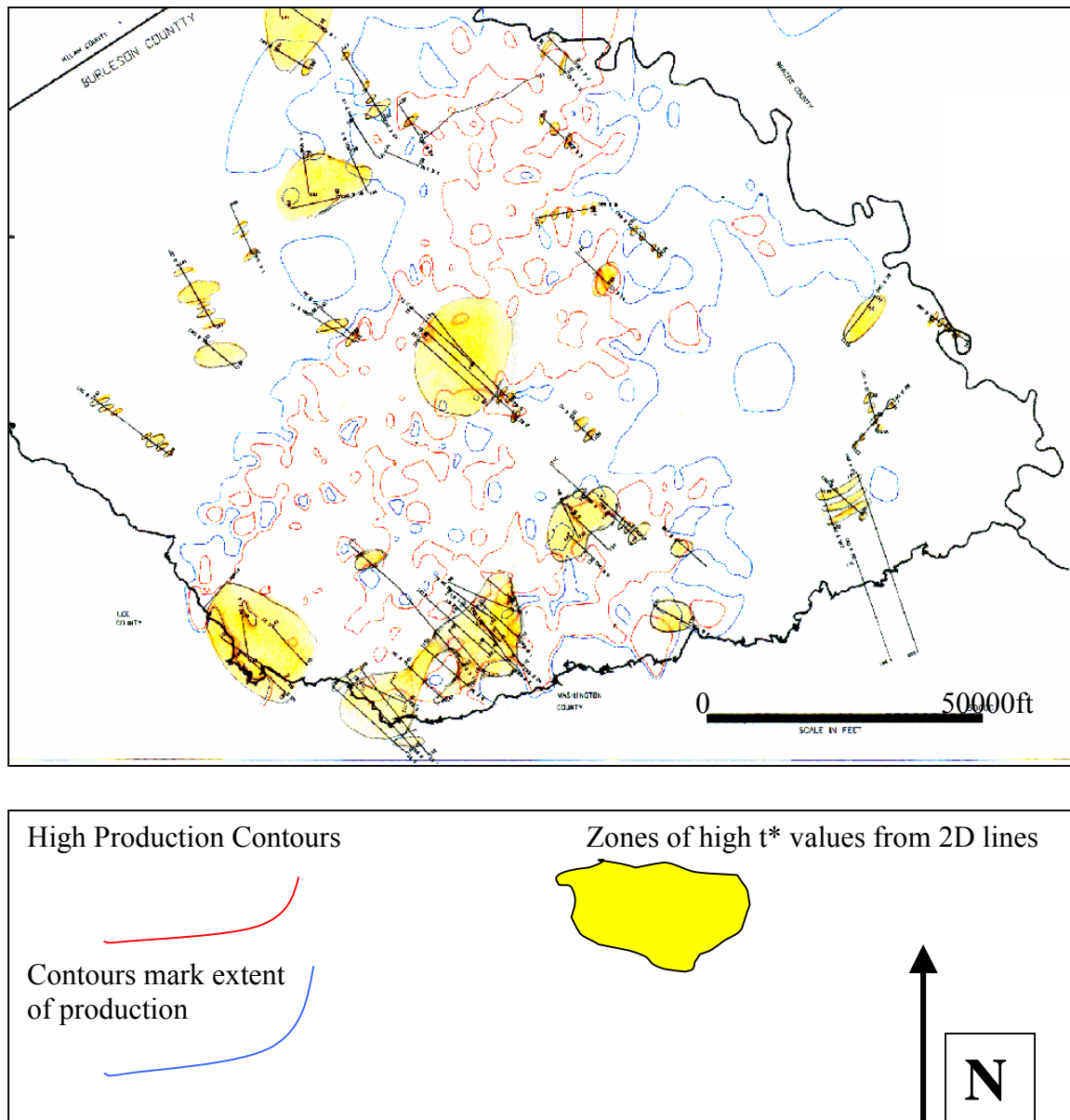Figure 14. t* attribute mapped over the study area derived from 2D data. The t*

attribute were computed from frequency spectra derived from 100ms windows above

and below the top of the Austin chalk reflector. Values were plotted along the 2D lines

and then contoured on the map. The cumulative production contours are plotted on this

map to show the correlation between production and t* attribute.
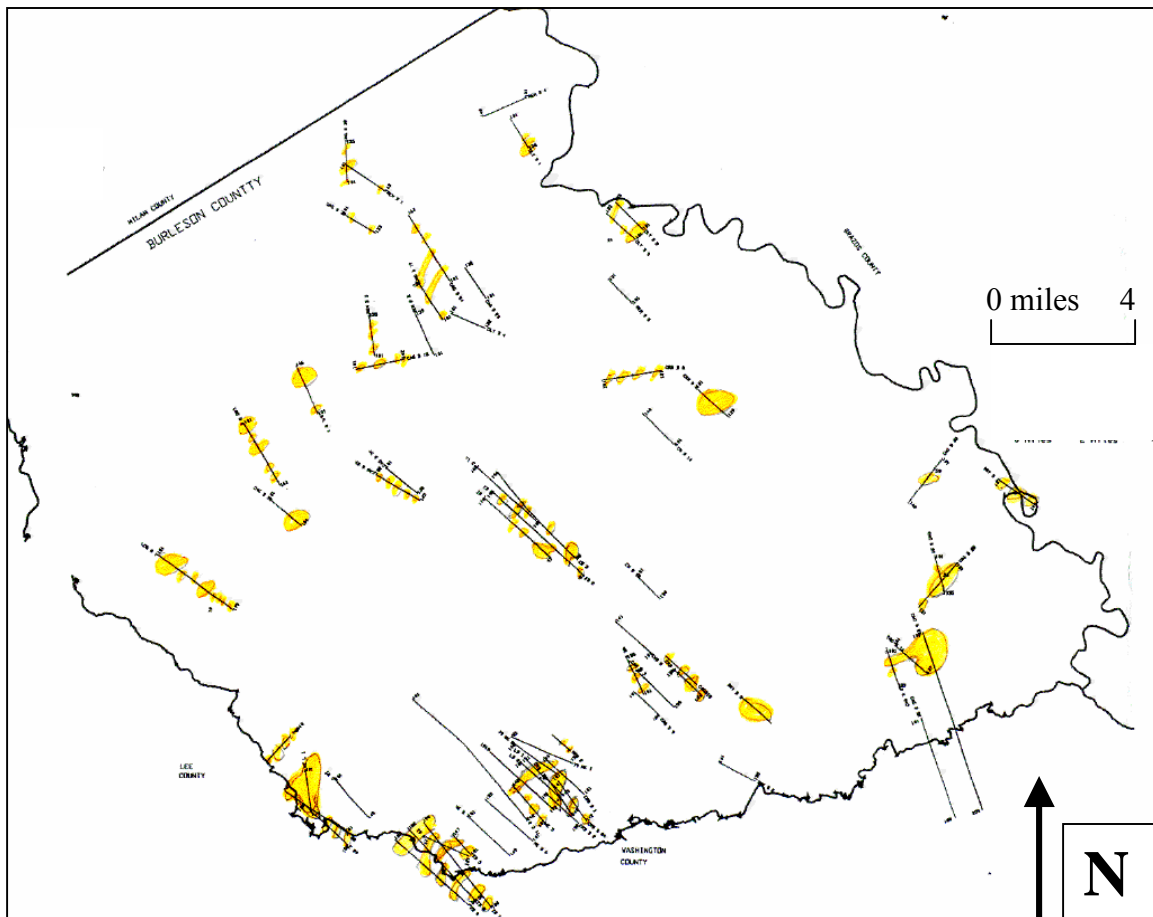
Figure 15. Amplitude anomalies (reduction in reflection amplitudes) that were interpreted on the 2D data are interpreted and plotted as yellow zones. There is no reflection magnitude anomalies interpreted on some 2D lines due to poor quality of the reflection magnitude data. The amplitude anomaly interpretation is not interpolated beyond the close vicinity of the 2D lines.

CASE STUDY: WALNUT CREEK 3D DATA SET

The Austin Chalk layer is faulted and the major fault trend is parallel to strike (Figure 16). Based on previous studies from borehole and production data, fracture orientations in the Austin Chalk are parallel to strike (Friedman et al., 1995, Corbett et al. 1987, Lewallen 1992).

INTERPRETATION

The faults were interpreted and show a general trend parallel to the strike of the Austin Chalk. A major fault runs across the survey area and divides the survey into two zones:

  1. The zone northwest of the major fault which is not faulted

  2. A highly faulted zone southeast of the major fault containing multiple faults.

The top of the Austin Chalk in the survey area dips southeast. On the updip side of the major fault, a small structural high appears to parallel the fault across. This would be a target area for drilling if it is found to be fractured (Figure 17).

FREQUENCY SPECTRA

The frequency spectra of the seismic traces are derived from each individual trace over a 100ms time window from above and below the interpreted Top of the Chalk horizon. These frequency spectra above and below the chalk are compared in Figure 18.

The attribute t* was derived for each of the three data volumes
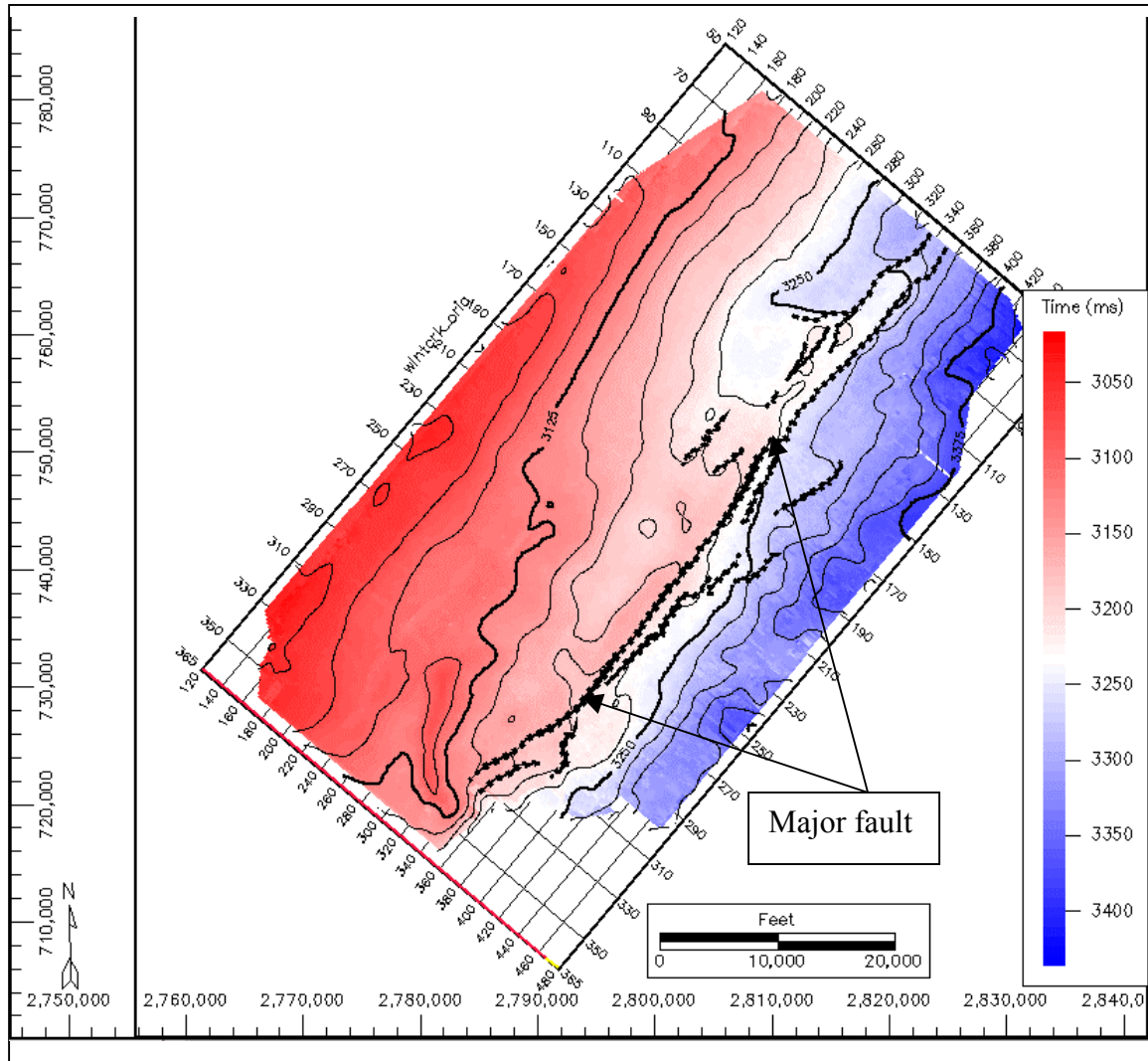
  1. Original data volume

Figure 16. Time-structure map of the TOC reflector. Data displayed on the Walnut
Creek data 3d survey grid. The regional dip is to the Sourtheast with the Inlines
oriented N50W - S50E parallel to the dip direction. The major fault trend displayed on
the surface is parallel to strike.
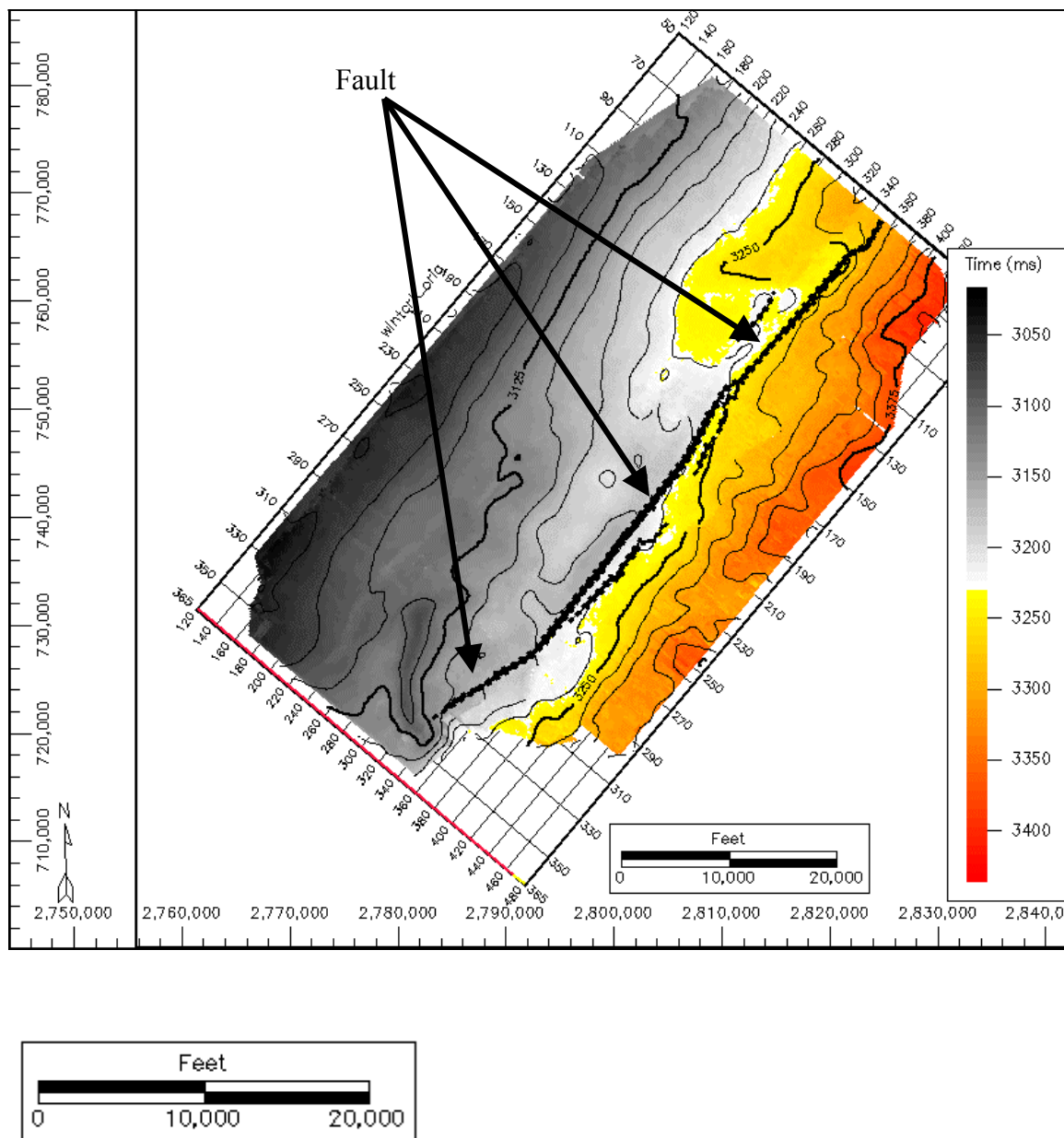
Figure 17. Fault boundaries interpreted on the TOC reflector. Data displayed on the Walnut Creek data 3d survey grid. The time contours are displayed to show the structural highs in the middle of the survey, marked by closed contours. The contour interval is 10ms. The major fault running across the survey is marked on the map.

Figure 18. Comparison of the frequency spectra for 100 ms time window (a) above the TOC and (b) below the BOC from the Walnut Creek 3D data. The shown sample trace is Line150 CDP300.

2.Perpendicular Azimuths volume

3. Parallel Azimuths volume

INTERPRETATION OF THE t* ATTRIBUTE VALUES

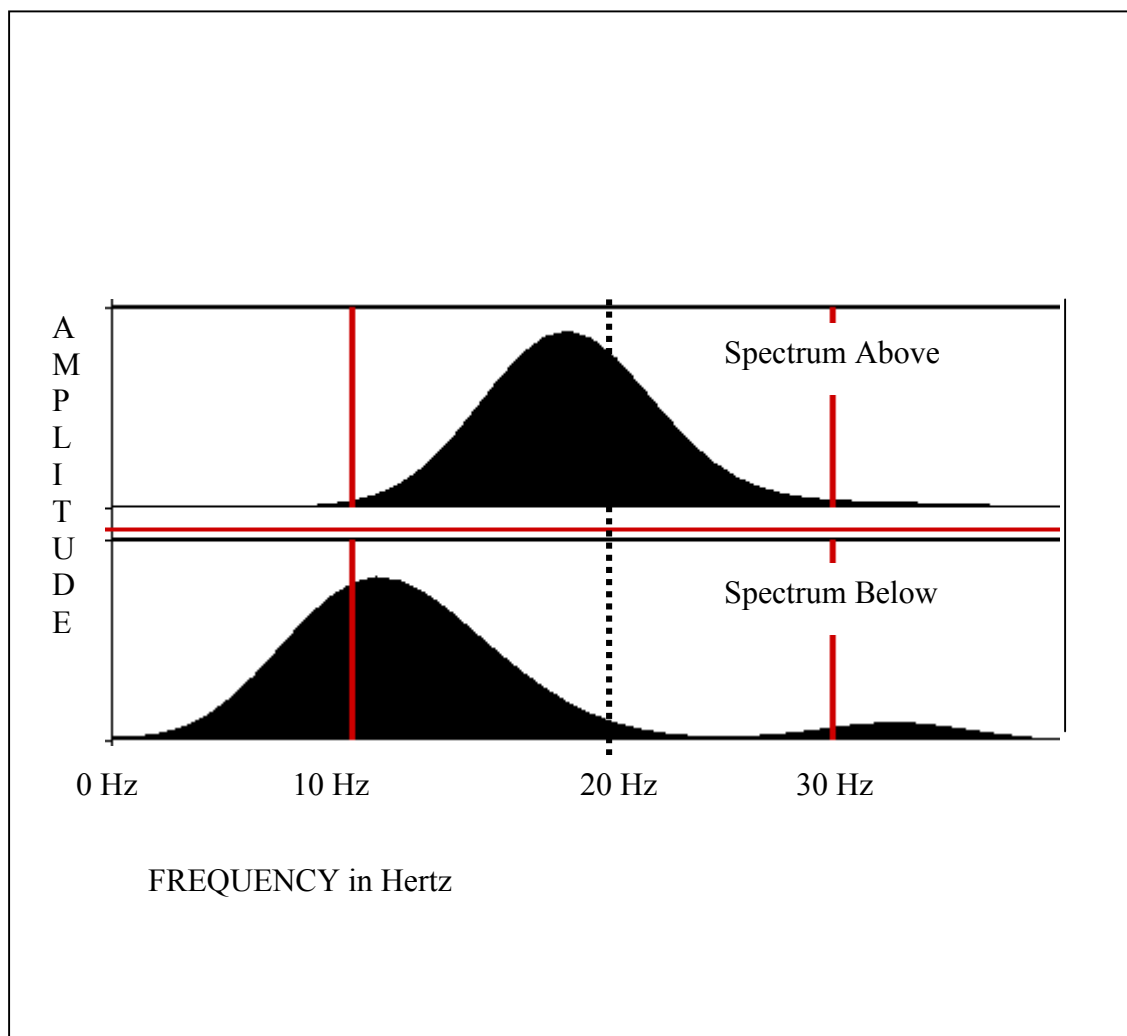Interpretation of the t* fracture indicator attribute is based on positive t* values being indicative of attenuation of higher frequencies. Larger t* values correspond to greater attenuation of higher frequencies and the shift of the spectra towards lower frequencies. This attenuation of higher frequencies is the fracture indicator.

Figure 19 and Figure 20 show that the entire data set and perpendicular azimuth volumes have high t* values that trend parallel to the faults. The t* values derived from perpendicular azimuth data shows a wider zone than the t* values derived from the entire data set. The high t* values that trend parallel to the strike of the Austin Chalk are interpreted to be fracture zones. The t* values derived from the parallel data set does not have this trend. Figure 21. This lends evidence to the major fracture orientation being parallel to strike.

There are some trends at an angle to strike in Figure 19 and coincide with faults suggesting a close relationship to faulting. The difference between Figure 19 and Figure 20 is given in Figure 22. The major trend of high t* values parallel to strike is still prominent in this figure. However, some smaller trends begin to emerge sub_parallel to strike. This suggests that there are several fracture orientation trends.
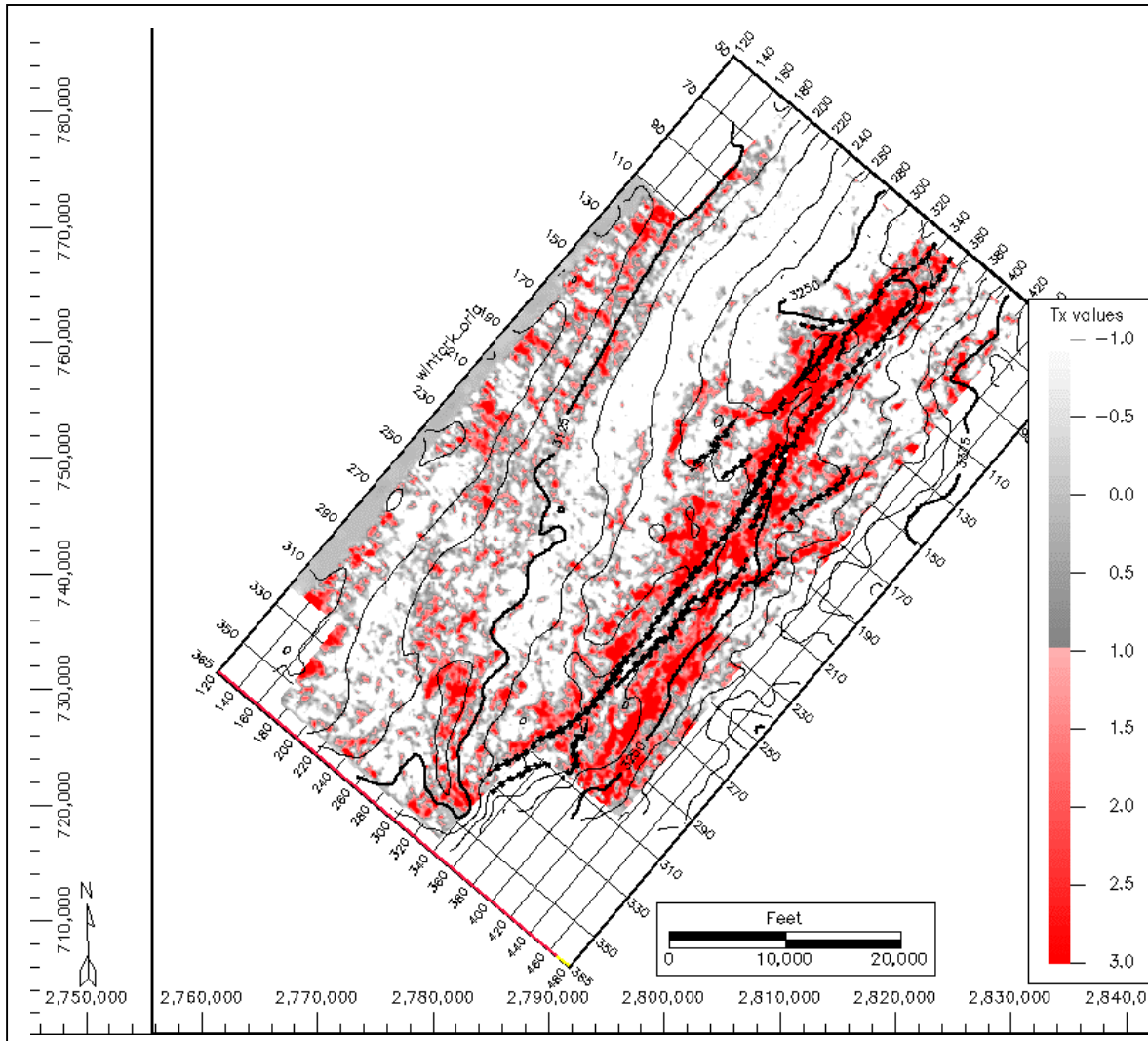
Figure 19. t* attribute derived from the entire data set (all azimuths) plotted on the survey. High values are plotted in darker colors and indicate attenuation of higher frequencies, which indicate fractures. The trend is parallel to both strike and to the faulting. The t* trend follows the fault trends and does not coincide with the crest of the structural highs (Figure 17). There are some trends that are not parallel to strike but coincide with the fault pattern suggesting a close relationship between fault and fractures.
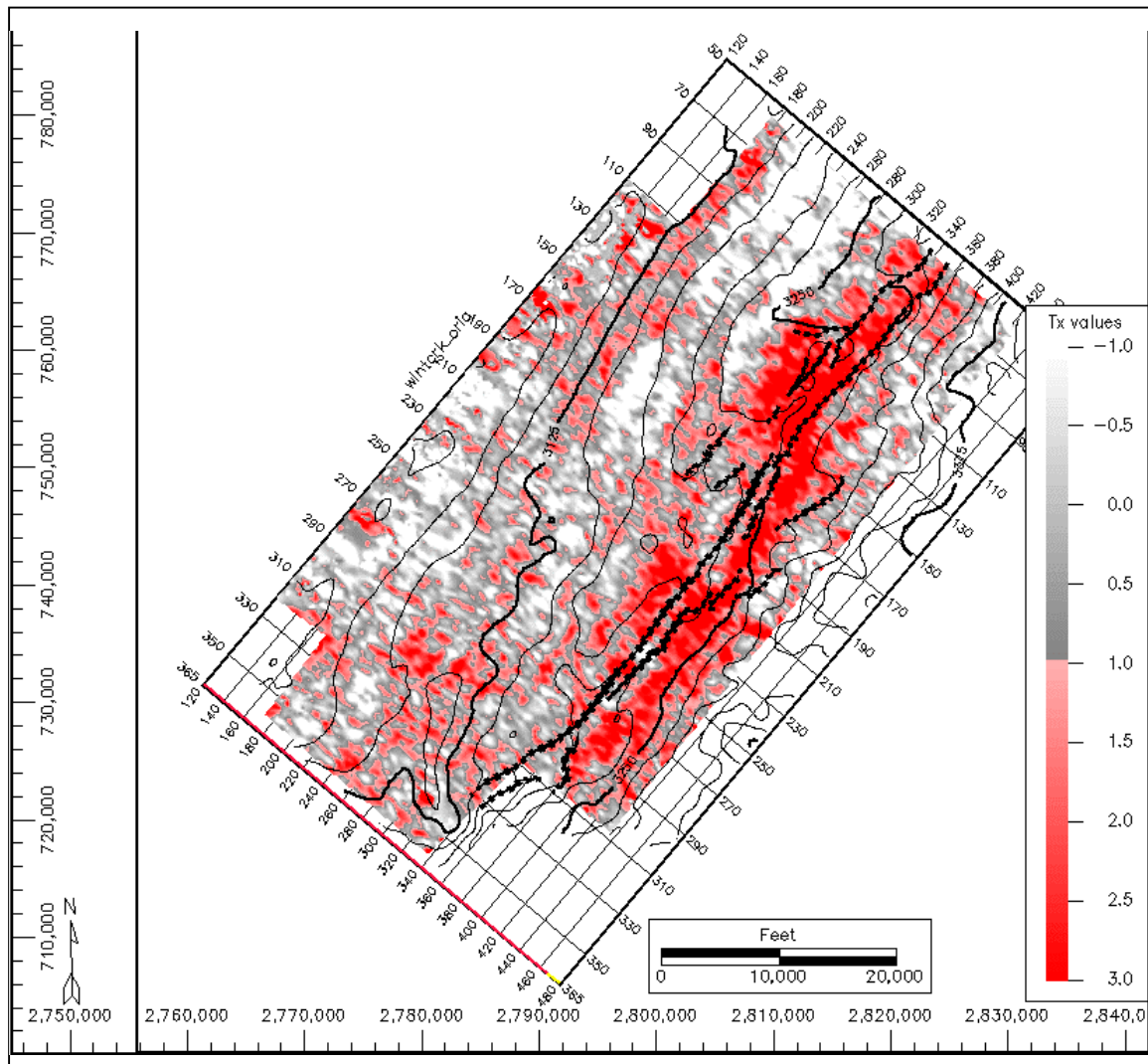
Figure 20. t* attribute derived from the perpendicular azimuth data set. High values

suggest fractures. The trend is parallel to both strike and to the faulting. Due to the

limited azimuth, features evident in Figure 19, at an angle to strike, are not evident

here. The similarity of the t* trend between Figure 19 and Figure 20 lends evidence to

fracturing being perpendicular to line direction. Once again the t* trend follows the

fault trend and does not correspond to the structural high.
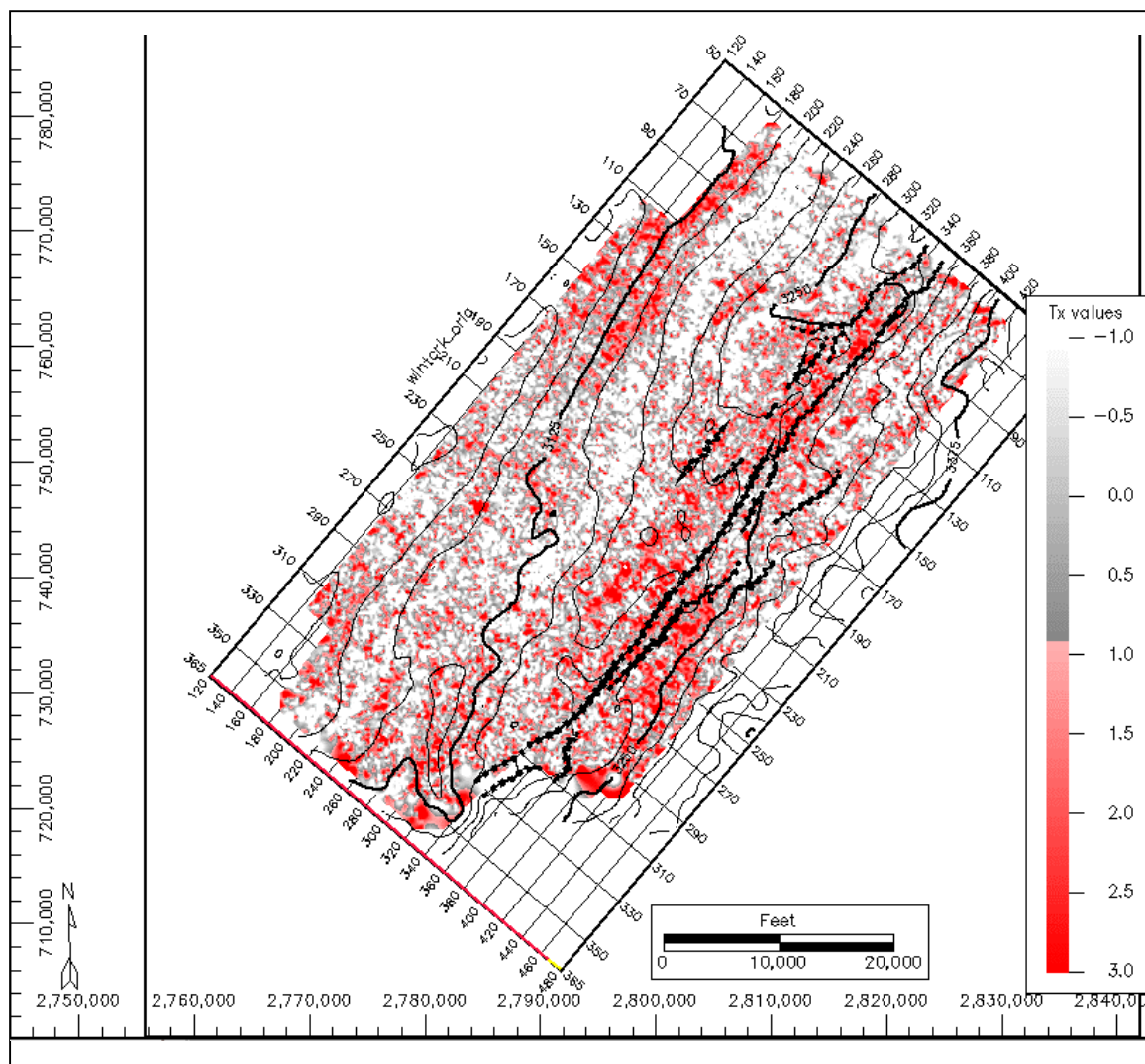
Figure 21. t* attribute derived from the parallel azimuth data. This is a comparison plot

with no prominent trend evident. The t* attribute do not show the attenuation as seen in

Figure 19 and Figure 20. The same range of values is used for the color spectra for

Figures 19, 20 and 21.

Figure 22. Difference of t* attribute. t* attribute from the perpendicular data subtracted

from t* attribute from the entire data set to bring out t* trends that are at an angle to the

strike direction. These residual trends are at approximately 30 degrees to the main

trend. There are no prominent trends perpendicular to the strike orientation.

Contribution to the attenuation of high frequencies, seen in the entire data set, is from all of these orientations. The perpendicular data set does not have these t* value trends.

SHIFT IN PEAK FREQUENCIES

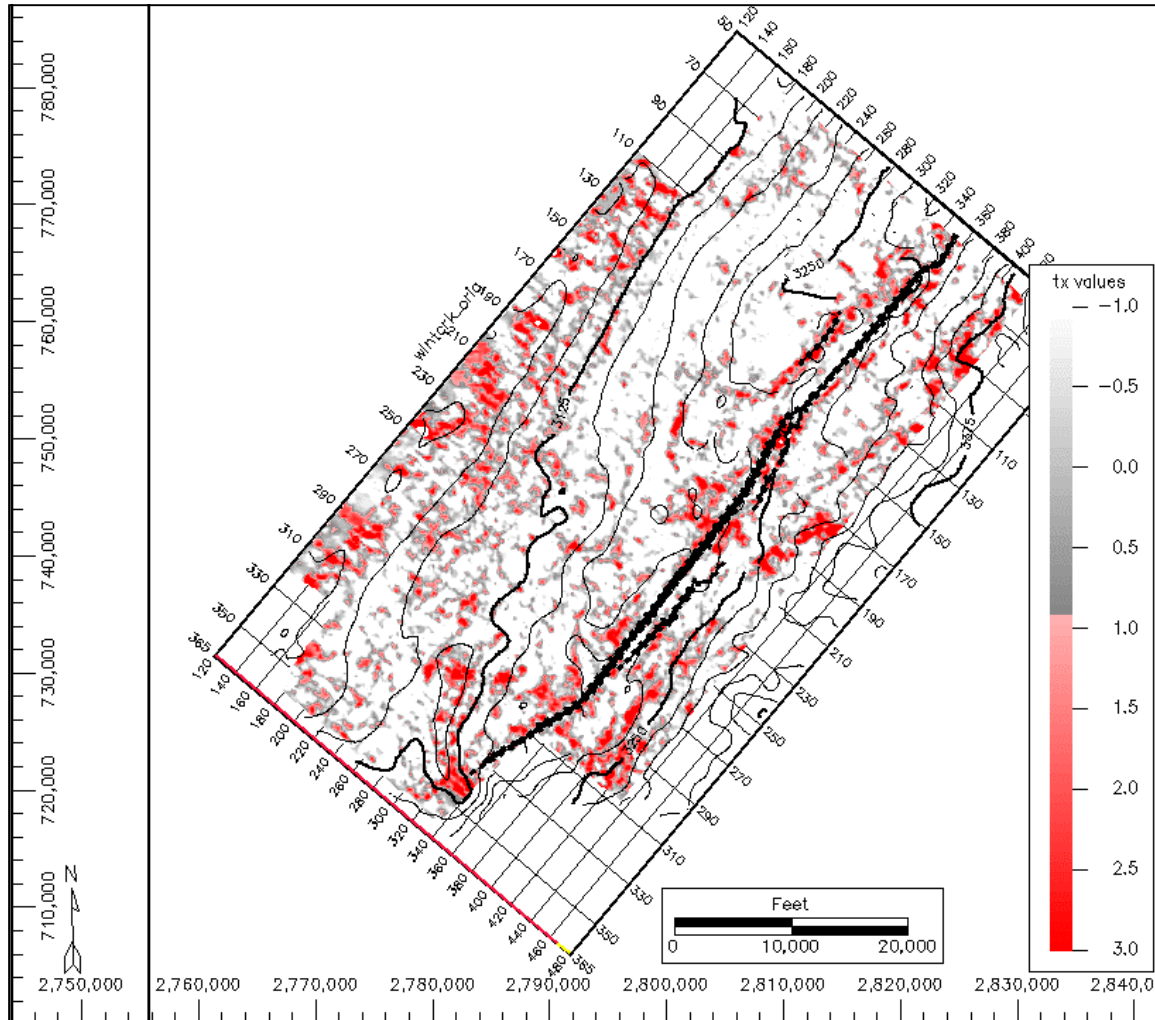The attenuation of higher frequencies is observed in the shift of frequency spectra towards lower frequencies. The 'Peak Frequency' is an additional attribute derived from the seismic traces. The amplitudes of higher frequencies are attenuated due to fracturing and therefore the value of the 'Peak Frequency' changes for spectra derived from time window above and below the chalk. An example is given in Figure 18. This change in value for the Peak Frequency is mapped as the shift in peak frequency in Figure 23. A greater shift in Peak Frequency indicates greater attenuation. The trend in Figure 23 correlates well with the t* data trend in Figure 19 and 20.

SWEET SPOTS

Based on the fracture indicator t* from Figure 20, the area recommended for a fracture reservoir would be in the northeastern half of the survey, northwest of the major fault, between lines 90 – 270 and CDP's 260 – 360. This outlines a region of high t* values which corresponds to a structural high seen in the time structure map in Figure 17.
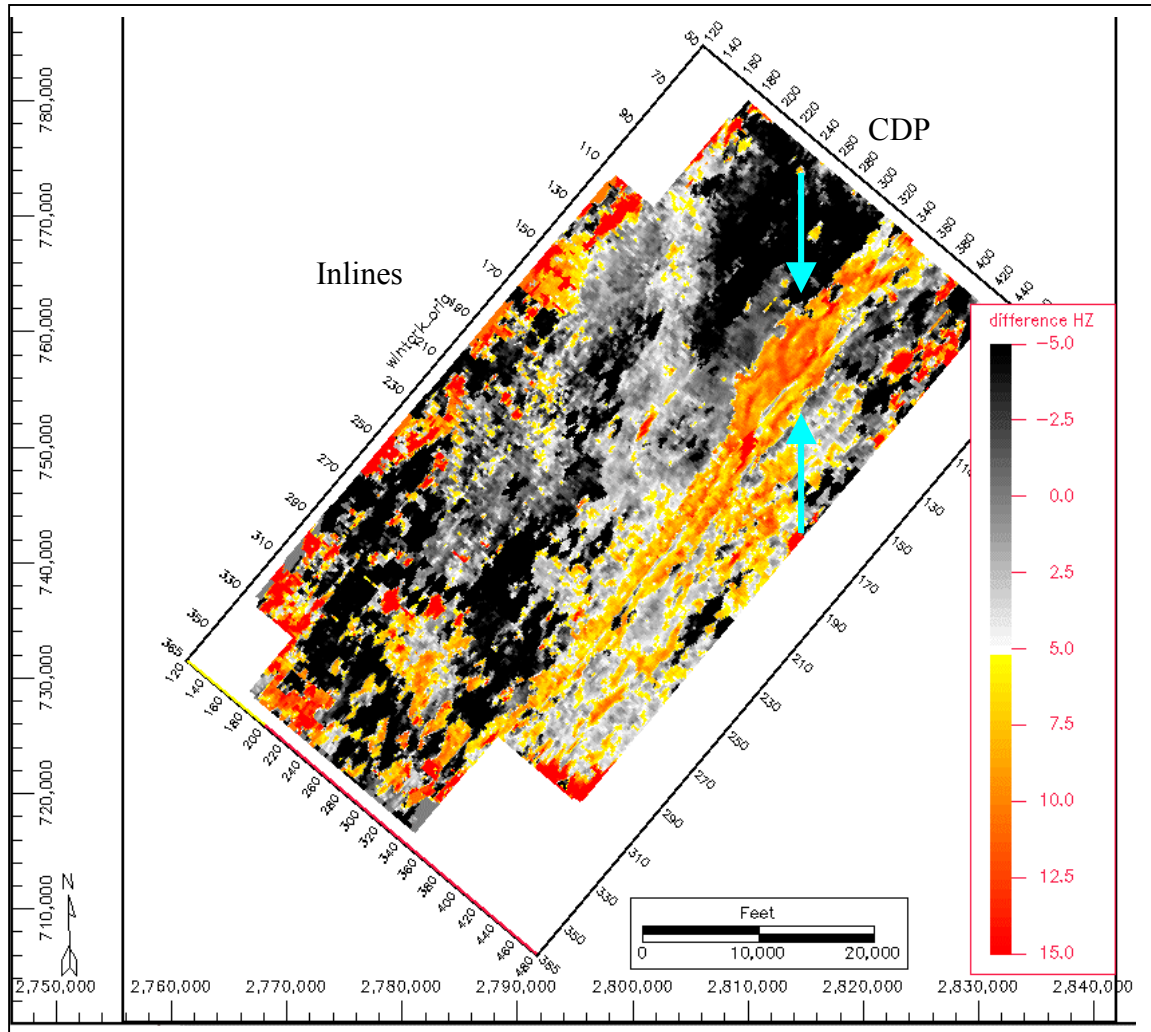
Figure 23. Shift in peak frequencies. The shift, or difference, in peak frequencies from spectra above and below the chalk calculated over the entire data set is plotted on the survey. Attenuation of higher frequencies is indicated by a positive difference in peak frequencies. The interesting feature is between Lines 70 and 170 and CDP's 310 and 370, which displays a similar linear trend parallel to strike, but with some subtle features at an angle to strike and dip.

The t* attribute shows that the fractured region continues onto the downthrown side of the fault and also stretches into the southwestern half of the survey as well. The downthrown side is highly faulted and therefore may not be a good choice for drilling targets.

APPLICATION OF METHOD TO THE EDWARDS BELOW THE AUSTIN CHALK

The t* attribute was calculated for the Edwards layer, that underlays the chalk in this area. A 100 ms window was used just below the Austin Chalk. This window covered the Edwards layer underneath. The results are given in Figure 24. The t* anomaly trend is parallel to strike and overlaps the same regions as Figures 19 and 20. The Edwards being a limestone could be fractured though not as extensively as the Austin Chalk. The fracturing in the Edwards may be controlled in part by the fracturing in the Austin Chalk from above. Contribution to the t* values (Figure 24) by the Austin Chalk cannot be ruled out, therefore, it is difficult to interpret this solely as fracture zones within the Edwards.

CONTROL CALCULATIONS ABOVE THE AUSTIN CHALK

A reflector was interpreted approximately 500 milliseconds above the top of the Chalk, and the same t* values derived from 100 millisecond time windows above and below this reflector. The values are plotted in Figure 25 with the same spectrum scale as those

in Figure 19, 20 and 21 for comparison. The t* values are within the 0.5 range, and indicate little frequency attenuation. No prominent trend in the t* attribute is evident.

AMPLITUDE ANOMALIES

The reflection magnitude on the Top of Austin chalk layer is displayed in Figure 26. The color scale was chosen to highlight the low amplitude anomalies. This figure displays the fault boundaries on the Top of Austin chalk. Figure 26 shows a good correlation between faults and low amplitudes.

CONCLUSIONS FROM THE WALNUT CREEK 3D DATA CASE STUDY

- The t* indicator is a qualitative fracture indicator.

- The shift in peak frequencies supports the evidence from the t* data evaluation.

- Correlation of t* attribute from the entire data volume and fracture orientation data from other studies indicates that the method works well with a conventional 3D data set.

- The attenuation of frequency due to fracturing is evident on azimuths perpendicular to the fractures but not evident on azimuths parallel to the fractures.

- Seismic data limited azimuthally helps in the derivation of the fracture indicator.
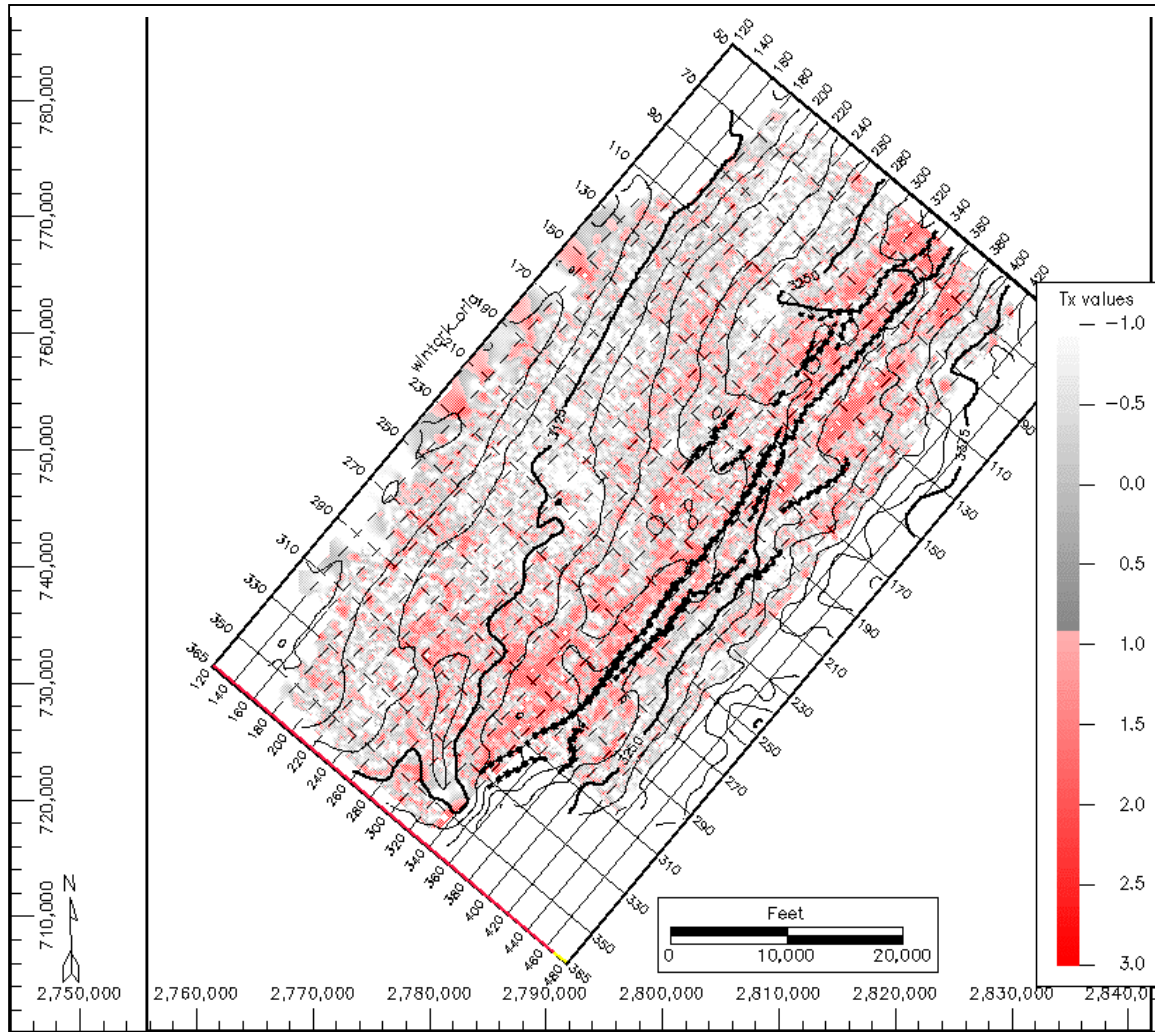
Figure 24. t* attribute values from the Edwards layer. t* attribute from a 100 ms

window covering the Edwards layer underneath the Chalk. The t* anomaly trend is also

parallel to strike and overlaps the same regions as Figures 19 and 20.
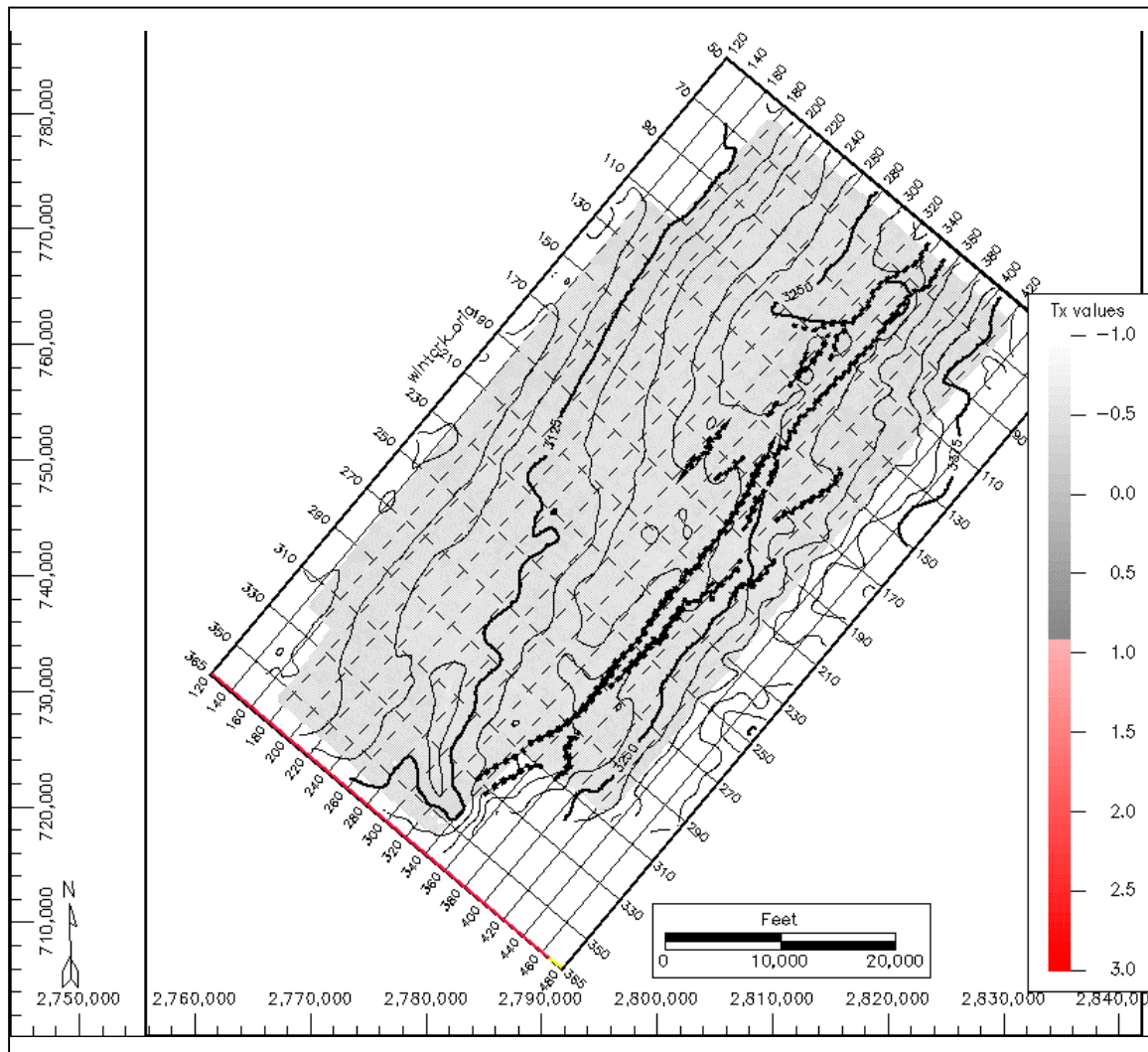
Figure 25. t* attribute derived from a reflector 500ms above the Austin Chalk. Similar

100ms windows from above and below this reflector were used to derive the spectra for

the computations. The results are displayed with the same scale to emphasize there is

very little attenuation of high frequencies within the combined 200 millisecond window

and that there are no prominent trends evident. This implies that this is not a fractured

interval.
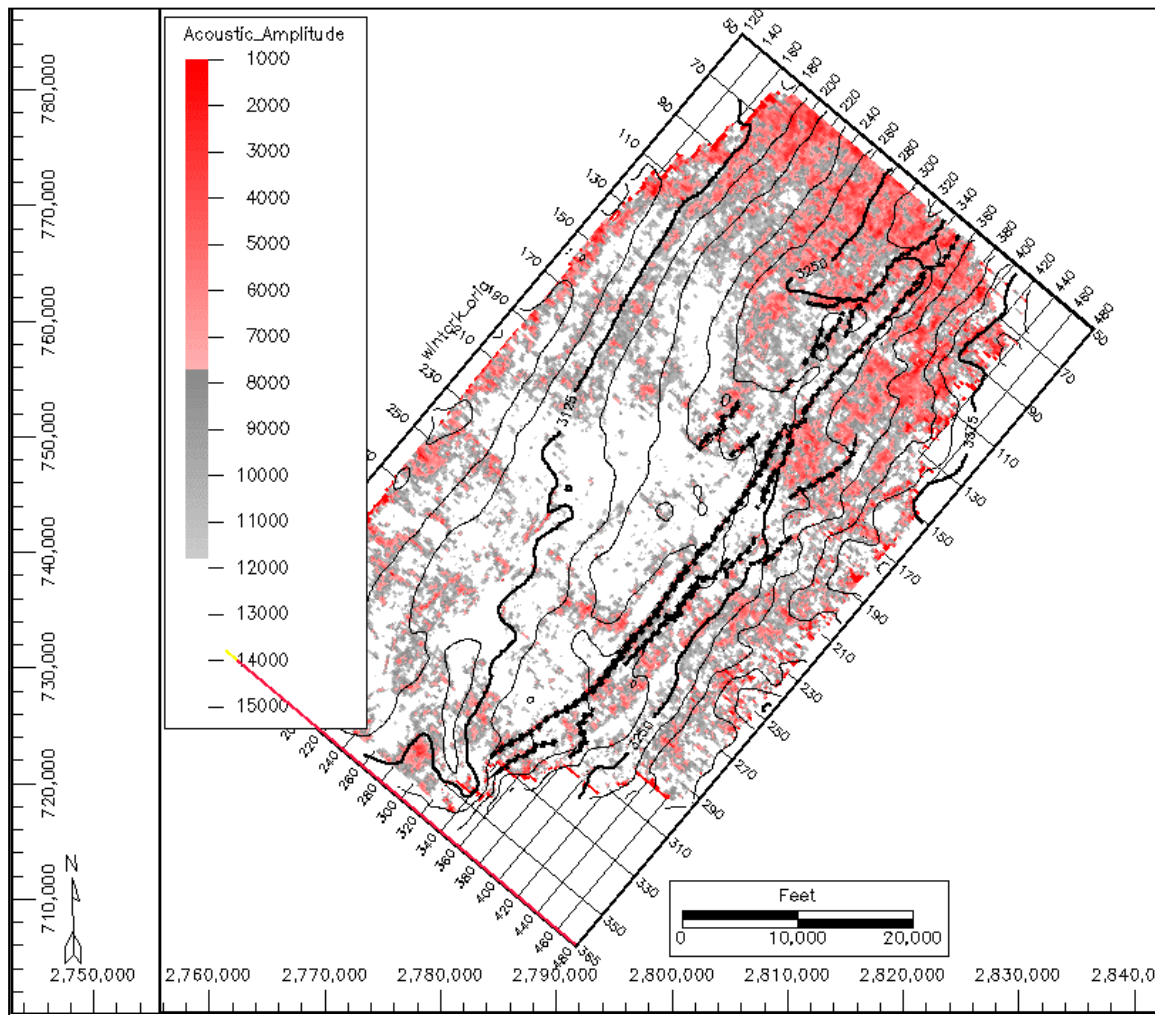
Figure 26. Fault boundaries overlying reflection magnitudes show the correlation
between the faulting and the low amplitude anomalies. There are some low amplitude
trends (that display the same general pattern over the area) which do not have faults
interpreted on them. This suggests that there might be faults that were overlooked, or
the low amplitudes anomalies indicate fractures not associated with faulting. The low
amplitudes on the edges of the survey are due to noise in the data.

- The interpretation of fracture orientation is along strike, as seen from the good correlation between the t* attribute from the original data volume and the perpendicular azimuth volume.

- Amplitude anomalies correlate well with the fault interpretation. Therefore, there is good correlation with the t* attribute. The amplitude anomaly extends beyond the fault on each side, suggesting that the fractures are not limited to the immediate vicinity of the faults but instead forms a zone of fractures next to the fault.

CONCLUSIONS

1. t* are consistent with production distribution in Burleson County and known fault distribution in Austin County data. These relationships support my conclusion that t* is a fracture indicator.

2. Fracture orientations observed on the 3D data case study show that the prominent trend is parallel to strike.

3. The fracture zones are best delineated by data with shot receiver geometries that are perpendicular to fracture orientation. Shot-receiver arrays parallel to the fracture orientation (parallel azimuths) do not see fractures perpendicular to the seismic line.

3. Azimuth volume data set with shot-receiver azimuths perpendicular to the fractures better indicates fracture zones within the Austin Chalk layer.

4. The comparison of frequency spectra shows the attenuation of higher frequencies.

5. The t* attribute in the northwestern part of Burleson County indicate fracture zones outside the zone of production. This may be due to the fact that it is outside the oil maturation window and does not contain hydrocarbons in economic quantities.

6.Amplitude anomalies also have a good correlation with both the fracture indicator t*

attribute and production data.

7.The attribute (t*) developed in this study is a qualitative fracture indicator to indicate

zones of fracturing using seismic P-wave data. It does not, however, give a

quantitative measure of the fracture density.

PROPOSED FUTURE WORK

The t* calculations can be applied to several shot receiver azimuth volumes generated from the original volume. Due to limitations in time and resources available for this study, only two azimuth volumes, parallel to strike and perpendicular to strike, were generated. The fracture indicator t* attribute from the original data set shows trends that would indicate fracture orientations at an angle to the major fracture orientation (parallel to strike). Rotating the shot receiver azimuths through several angles would give a comprehensive picture on different fracture orientations and further validate the major fracture orientation direction.

A regular grid of closely spaced 2D lines would give better coverage over the exploited areas. The fault and fracture trends would be better mapped in the Austin Chalk, and interpretation could be interpolated between lines.

Prestack data was not used in this study. An additional area of study would be to look at the frequencies and the attenuation of higher frequencies in prestack data. This would allow the grouping of data in combinations of shot-receiver azimuths as well as reflection angles. (For example: Near Offset Stacks and Far Offset Stacks.)

REFERENCES

Al-Mustafa, H.,1992, Comparison of Compressional and Shear Wave Data in a Fractured Reservoir, M.S. Thesis, Texas A&M University, College Station, Texas.

Al-Shuhail, A.A., 1998, Seismic Characterization of Fracture Orientation in the Austin Chalk Using Azimuthal P-Wave AVO, Ph.D. Dissertation, Texas A&M Universtiy, College Station, Texas.

Anderson, D.L., Minster B., and Cole D., 1974, The effects of oriented cracks on seismic velocitites, Journal of Geophysical Research, **79**, 4011-4015.

Carmichael, R.S., 1981, Handbook of physical properties of rocks: C.R.C. Press.

Cloud, K.W., 1975, The Diagenesis of Austin Chalk, M.S. Thesis, Texas A&M University. College Station, Texas.

Corbett, K., Friedman, M., and Spang, J., 1987, Fracture development and mechanical stratigraphy of Austin Chalk, Texas: AAPG Bull., **71**, 17-28.

Corbett, K. P., 1982, Structural Stratigraphy of the Austin Chalk, M.S. Thesis, Texas A&M University, College Station, Texas.

Crampin, S., Lynn, H.B. And Booth, D.C., 1989, Shear-wave VSPs: A powerful new tool for fracture and reservoir description, J. Petr. Tech., **5**, 283-288.

Ewing, T.E., 1983, Austin/Buda fractured chalk. In W.E. Galloway (eds.), Atlas of major Texas oil reservoirs: Austin Texas. University of Texas Bureau of Economic Geology.

Friedman, M., and McKiernan, D. E., 1995, Extrapolation of fracture data from outcrops of the Austin Chalk in Texas to corresponding petroleum reservoirs at depth, J. Can. Petr. Tech., **34**, 43-49.

Gibson, R.L., Theophanis S., and Toksoz M.N., 2000, Physical and numerical modeling of tuning and diffraction in azimuthally anisotropic media, Geophysics, **65**, 1613-1621.

Guigne J. Y., Pace G. N. and Chin V. H., 1989, Dynamic extraction on sediment attenuation from subbottom acoustic data, Journ. of Geoph. Res., **94**, 5745-5761.

Haugen, G.U., and Schoenberg, M.A., 2000, The echo of a fault or fracture, Geophysics, **65**, 176-189.

Hinds, G. S., and Berg, R. R., 1990, Estimating organic maturity from well logs, Upper Cretaceous Austin Chalk, Texas Gulf Coast, GCAGS Trans., **40**, 295-300.

Hudson, J.A., 1981, Wave speeds and attenuation of elastic waves in material containing cracks, Geophys. J. Roy. Astr. Soc., **64**, 133-150.

Hudson, J. A., 1988, Seismic wave propagation through material containing partially saturated cracks, Geophysical Journal, **92**, 33-37.

Lewallen, K. T., 1992, Identification of subsurface fractures in the Austin Chalk using vertical seismic profiles, M.S. Thesis, Texas A&M University, College Station, Texas.

Liu E., Crampin S., and Hudson J.A., 1997, Diffraction of seismic waves by cracks with application to hydraulic fracturing, Geophysics, **62**, 253-265.

McCann C., and McCann D.M., 1985, A theory of compressional wave attenuation in noncohesive sediments, Geophysics, **50**, 1311-1320.

Najmuddin, I., 2001, Frequency attenuation - a fracture indicator, Houston Geol. Soc. Bull., **43**, 7, 25 - 28.

Najmuddin, I., 2001, Detecting fracture zones in the Austin Chalk using seismic P-wave data, Houston Geol. Soc. Bull., **44**, 1, 22-27.

Richards, P.G. and Menke, W., 1983, The apparent attenuation of a scattering medium, Bull. Seis. Soc. Am., **73**, 1005-1021.

Schlumberger Educational Services, 1989, Log interpretation, principles/applications.

Schoenberg, M.S., Douma, J., 1988, Elastic wave propagation in media with parallel fractures and aligned cracks, Geophysical Prospecting, **36**, 571-590.

Snyder, R. H., and Craft, M., 1977, Evaluation of Austin and Buda formations from core and fracture analysis, GCAGS Trans., **27**, 376-385.

Tyler, N., Ewing, T., Galloway, W. E., Garrett, C. M. and Posey, J. S., 1983, Oil accumulation and production characteristics in major Texas oil reservoirs, 53rd Ann. Internat. Mtg., Soc. Expl. Geophys., Session:AAPG.4

VITA

Ilyas Juzer Najmuddin: Date of Birth 6th September 1966.

Nationality: Indian

Current Address: 17511 Coventry Squire, Houston, Texas, 77084.

Phone (281) 856 0126, Fax (281) 856 0403

Email: ilyasjn@houston.rr.com

Currently employed by: Schlumberger Information Solutions

Oilfield Services, Senior Geoscientist in Houston.

Phone (713) 513 2000

Email: inajmuddin@houston.oilfield.slb.com

Previous Degrees:

Master of Science in Geophysics 1993: University of Houston, Houston, Texas.

Bachelor of Science in Geophysics 1987: Cairo University, Cairo, Egypt.

Publications:

An Aeromagnetic Survey over the Eastern Deep Gulf of Mexico, Journal of Geophysical Research, 1994.

Frequency Attenuation: A Fracture Indicator, HGS Bulletin, May, 2001.

Detecting Fractures Using Frequency Attenuation, HGS Bulletin, September 2001.

Languages: English, Arabi, Urdu, Hindi, Gujarati.